Chung *et al.*
Cell Communication and Signaling (2024) 22:218
https://doi.org/10.1186/s12964-024-01572-3

Cell Communication and Signaling

RESEARCH

Open Access

Inhibition of adenylyl cyclase by GTPase-deficient $G\alpha_i$ is mechanistically different from that mediated by receptor-activated $G\alpha_i$

Yin Kwan Chung[1,3†], Ho Yung Chan[1†], Tung Yeung Lee[1] and Yung Hou Wong[1,2*]

Abstract

Signal transduction through G protein-coupled receptors (GPCRs) has been a major focus in cell biology for decades. Numerous disorders are associated with GPCRs that utilize G_i proteins to inhibit adenylyl cyclase (AC) as well as regulate other effectors. Several early studies have successfully defined the AC-interacting domains of several members of $G\alpha_i$ by measuring the loss of activity upon homologous replacements of putative regions of constitutive active $G\alpha_i$ mutants. However, whether such findings can indeed be translated into the context of a receptor-activated $G\alpha_i$ have not been rigorously verified. To address this issue, an array of known and new chimeric mutations was introduced into GTPase-deficient Q204L (QL) and R178C (RC) mutants of $G\alpha_{i1}$, followed by examinations on their ability to inhibit AC. Surprisingly, most chimeras failed to abolish the constitutive activity brought on by the QL mutation, while some were able to eliminate the inhibitory activity of RC mutants. Receptor-mediated inhibition of AC was similarly observed in the same chimeric constructs harbouring the pertussis toxin (PTX)-resistant C351I mutation. Moreover, RC-bearing loss-of-function chimeras appeared to be hyper-deactivated by endogenous RGS protein. Molecular docking revealed a potential interaction between AC and the α3/β5 loop of $G\alpha_{i1}$. Subsequent cAMP assays support a cooperative action of the α3/β5 loop, the α4 helix, and the α4/β6 loop in mediating AC inhibition by $G\alpha_{i1\text{-}i3}$. Our results unveiled a notable functional divergence between constitutively active mutants and receptor-activated $G\alpha_{i1}$ to inhibit AC, and identified a previously unknown AC-interacting domain of $G\alpha_i$ subunits. These results collectively provide valuable insights on the mechanism of AC inhibition in the cellular environment.

Keywords AC inhibition, G protein-coupled receptor, Receptor activation, Effector recognition domain, Constitutively active mutants

†Yin Kwan Chung and Ho Yung Chan contributed equally to this work.

*Correspondence:
Yung Hou Wong
boyung@ust.hk
Full list of author information is available at the end of the article

Introduction

G protein-coupled receptors (GPCRs) constitute a major class of cell surface receptors with characteristic 7-transmembrane helices. A plethora of diverse cellular activities that ranges from transcription [1], secretion [2], to cell migration [3] and proliferation [4] are orchestrated by GPCRs and their associated G proteins. Many GPCRs that signal through members of the G_i family have tremendous therapeutic value because they serve as key detectors and regulators in various physiological systems. For instance, G_i-coupled opioid receptors are the primary targets for opiate analgesics and their prolonged activation will inevitably lead to opiate tolerance and physical dependence [5]. Likewise, altered expression or function of G_i-coupled receptors are associated with various psychiatric disorders [6] including the serotonin $5\text{-}HT_{1B}$ receptor in depression [7], dopamine D_2 receptor in bipolar disorder [8], and α_{2A}-adrenergic receptor in schizophrenia [9]. Dysregulated G_i-coupled receptor signaling can also result in other chronic ailments such as inflammatory bowel disease [10], Alzheimer's disease [11], and heart failure [12].

Although many G_i-coupled receptors are capable of regulating multiple signaling pathways, they invariably inhibit adenylyl cyclase (AC) via both pertussis toxin (PTX)-sensitive and PTX-insensitive members of the $G\alpha_i$ subfamily (namely, $G\alpha_{i1\text{-}3}$ and $G\alpha_z$) [13, 14]. The molecular basis by which these $G\alpha_i$ subunits inhibit AC, however, has not been completely elucidated. Distinct preference for specific $G\alpha_i$ subunits has been reported for several GPCRs [15, 16], but there is little indication on whether such preferences have a determining effect on agonist-induced inhibition of AC. It remains to be established if $G\alpha_{i1\text{-}3}$ and $G\alpha_z$ utilize the same structural domains to interact with AC. Early chimeric studies have utilized GTPase-deficient mutants (mutation of the conserved Arg or Gln in the GTPase domain into Cys or Leu, respectively; henceforth referred to as RC or QL mutants) to map the effector-binding domains of $G\alpha_{i2}$ and $G\alpha_z$ [17–19], because replacement of the critical effector recognition domains on the mutants with homologous regions from other Gα subunits would abolish their constitutive inhibitory action on AC. These studies have provided valuable clues on the general location of the AC recognition domain in spite of a lack of $G\alpha_i$-AC structural data. The putative AC interaction domain of $G\alpha_{i2}$ was mapped across the switch II, α3 helix, α3/β5 loop and the α4/β6 loop [17, 18], with the latter structure in $G\alpha_z$ similarly implicated in effector recognition [19]. While the putative AC-interacting regions identified in these $G\alpha_i$ subunits are in line with the known effector domains of other Gα subunits such as $G\alpha_s$ [20], the precise molecular determinants for AC inhibition by $G\alpha_i$ remain elusive. A recent structural study on $G\alpha_{t1}$ and $G\alpha_s$ have further implicated the involvement of the αG/α4 loop in effector recognition [21]. A phenylalanine residue (F283) on the αG/α4 loop of $G\alpha_{t1}$ is seemingly essential for effector activation, and mutation of the cognate residue (F312) on $G\alpha_s$ also abolishes the activity of $G\alpha_s$QL [21].

The interchangeable use of RC and QL mutants in various experiments, including the early mapping studies [17–19], assumes that both GTPase-deficient mutants behave similarly. Yet, several reports have hinted at potential functional differences between the two mutations. For instance, an I25A mutation on $G\alpha_q$ was shown to eliminate the constitutive stimulation of phospholipase Cβ (PLCβ) by the RC, but not the QL, mutant [22]. Another study on the oncogenic potentials of constitutively active $G\alpha_i$ mutants observed that only mutation on Gln204, but not Arg178, of $G\alpha_{i1}$ suppressed cAMP formation in NIH/3T3 fibroblasts [23]. Moreover, GTP hydrolysis of $G\alpha_{i1}$RC, but not $G\alpha_{i1}$QL, was accelerated by RGS4 (a regulator of G protein signaling) when assayed with purified recombinant proteins [24]. These provided clues that QL and RC mutations may have intrinsic differences which have been overlooked in earlier studies, even though they both impede GTP hydrolysis and result in constitutive activation of the Gα subunits. Fundamentally, the extent to which the two constitutively active mutants resemble a receptor-activated Gα subunit, which is more physiologically relevant, have not been carefully examined.

Given that activated $G\alpha_i$ members are known to interact with proteins other than AC, such as regulators of G protein signaling (RGS) proteins [25] and G protein regulated inducer of neurite outgrowth 1 [26], it is pertinent to identify residues that specify distinct signaling or regulatory outcome. Hence, in the present study, a series of $G\alpha_{i1}$ chimeras with the putative effector-interacting domains replaced by homologous regions of $G\alpha_{t1}$ or $G\alpha_q$ were constructed with or without a GTPase-deficient mutation (QL or RC), and the chimeras were tested for their ability to abolish the constitutive activity. The reasons of choosing $G\alpha_{i1}$ as a model to examine QL and RC mutations are multifold. Firstly, functional difference between $G\alpha_{i1}$QL and $G\alpha_{i1}$RC have been reported [23, 24]. Secondly, $G\alpha_{i1/t1}$ chimeras were extensively used for deciphering effector-binding regions of transducin [21, 27, 28]. Mapping studies on $G\alpha_{i2}$, which shares > 90% homology with $G\alpha_{i1}$, also provide clues on putative AC-interacting domains of $G\alpha_{i1}$ [17, 18]. Thus, the activities of $G\alpha_{i1}$ chimeras harboring the QL or RC mutation can be readily tested to infer the functionality of the two mutants. Our results clearly suggest that there exist functional differences between $G\alpha_{i1}$QL and $G\alpha_{i1}$RC, and that the receptor-driven active conformation of $G\alpha_{i1}$

is functionally more efficient than GTPase-deficient mutants of $G\alpha_{i1}$ in suppressing the activity of AC. Moreover, we identified α3/β5 loop as an additional region generally utilized by $G\alpha_{i1-3}$ for AC inhibition. These findings shed light on the mechanism of $G\alpha_i$ to elicit its effect in a biological context upon receptor activation.

Results

Design and expression of $G\alpha_{i1}$ chimeras

Although the AC-interacting domains of $G\alpha_{i1}$ have not yet been elucidated, designing an effector-deficient $G\alpha_{i1}$ chimera to test for abolishment of QL/RC-driven constitutive activities was made feasible by previous mutagenesis and structural studies of other Gα subunits (such as $G\alpha_{i2}$), because $G\alpha_{i1-3}$ show remarkably high homology (~90% with respect to $G\alpha_{i1}$) [29]. Moreover, several regions identified in previous mapping studies [17–19, 27, 30] correspond to potential effector binding sites in the crystal structures of $G\alpha_{t1}$ and $G\alpha_s$ [20, 31]. These domains include the switch II region, switch III region, α3 helix, αG/α4 loop, α4 helix and the α4/β6 loop, and molecular modeling of $G\alpha_{i1}$ revealed that they may provide a planar surface for protein–protein interaction (Fig. 1A). It is likely that $G\alpha_{i1}$ employs one or more of these regions to interact with AC.

Since $G\alpha_{t1}$ and $G\alpha_q$ share approximately 60% homology with $G\alpha_{i1}$ but do not interact with AC, they have been proven as suitable partners for generating chimeras with $G\alpha_i$ subunits [17, 27]. A series of $G\alpha_{i1}$ chimeras were constructed (Fig. 2A) with one or more of their putative effector recognition domains substituted by homologous regions of $G\alpha_{t1}$ (Chi1-4) or $G\alpha_q$ (Chi5-6). We began by swapping the entire α4 helix to the α4/β6 loop of $G\alpha_{i1}$ (residues 297–318) with the homologous region of $G\alpha_{t1}$ to form Chi1 (referred to as Chi3 in [27]) (Fig. 2A). This domain was previously demonstrated to be important for AC inhibition by $G\alpha_{i2}$ [17, 18] and $G\alpha_z$ [19]. Chi2 was created by an additional swapping in the switch III region (referred to as Chi7 in [27]). This chimera was found to interact with phosphodiesterase γ (PDEγ) as efficiently as $G\alpha_{t1}$ [27], and therefore may have switched its effector preference from AC into PDEγ. Chi3 was constructed with the $G\alpha_{t1}$ sequence in Chi1 extended up to the C-terminus (Fig. 2A) because an equivalent chimera (named as zt295) using $G\alpha_z$QL as the backbone resulted in a loss of the constitutive AC inhibition [19]; the AC-inhibiting surface of $G\alpha_{i1}$ might be similarly affected in Chi3. Chi4 (also referred to as Chi4 in [27]), was designed such that both the switch III region and the C-terminal region starting from the α4 helix of $G\alpha_{i1}$ were swapped with that of $G\alpha_{t1}$ (Fig. 2A). Similar to Chi2, this chimera was previously shown to interact with PDEγ, which suggests that the effector specificity of the Chi4 is geared towards PDEγ [27]. Chi5 and Chi6 were equivalent to Chi1 and Chi3, except $G\alpha_q$ sequence was used to replace the targeted segments of $G\alpha_{i1}$ (Fig. 2A). As $G\alpha_q$ has a lower overall homology to $G\alpha_{i1}$ than $G\alpha_{t1}$ [29], it is expected that such replacement would be more effective than $G\alpha_{t1}$ in abolishing the activity of the GTPase-deficient mutations. In addition, Chi6 has retained the last 5 residues of the $G\alpha_{i1}$. Retainment of the last 5 residues of $G\alpha_i$ would allow subsequent examination of the chimera for activation by G_i-coupled receptor [32].

We have additionally incorporated several point mutations that have previously been found to be important for effector interactions in selected chimeras (Figs. 1B and 2A). Two residues on the α3 helix of $G\alpha_{t1}$ (H244 and N247; equivalent to K248 and D251 in $G\alpha_{i1}$) are critical albeit not sufficient for conferring its activity [28], but full activity can be attained in association with another residue (F283) on the αG/α4 loop [21]. Since this latter residue is also critical for the stimulatory activity of $G\alpha_s$ [21], it may represent an important determinant for interaction between $G\alpha_{t1}$/PDEγ and $G\alpha_s$/AC. Unlike $G\alpha_{t1}$ and $G\alpha_s$, $G\alpha_{i1}$ possesses the more polar Y287 at the corresponding location (Fig. 1B). Hence, combinatorial replacement of K248, D251, and Y287 by cognate residues of $G\alpha_{t1}$ (Fig. 2A) may impair the AC-inhibiting ability of the $G\alpha_{i1/t1}$ chimeras. Another study on the effector-interacting domain of $G\alpha_q$ revealed the importance of three consecutive residues in the switch III region (DNE motif, homologous to EEM in residues 238–240 of $G\alpha_{i1}$) [33]. Owing to a conserved structure across all Gα subunits, it is possible that AC interaction will be eliminated when these three residues on Chi1 are all substituted by alanine (resulting in Chi1-AAA; Fig. 2A). All chimeras were expressed at levels comparable to parental $G\alpha_{i1}$ in transiently transfected HEK293 cells (Fig. 2B).

(See figure on next page.)

Fig. 1 Putative AC-interacting domains of $G\alpha_{i1}$. **A** The 3-dimensional structures of the GTPase domains of inactive (gray, PDB code: 1GP2) and active $G\alpha_{i1}$ (yellow, PDB code: 1GFI) are overlaid and displayed as side, top and expanded views. The putative AC-interacting domains are marked in pale green (for side and top views) or labeled in the expanded view. Residues that are strictly conserved in AC-inhibiting $G\alpha_{i1-3}$ and $G\alpha_z$ are shown as cyan (inactive) or orange (active) sticks in the expanded view. **B** Amino acid sequence alignment of the putative AC-inhibiting regions between $G\alpha_{i1-3}$, $G\alpha_z$, and the homologous regions of $G\alpha_{t1}$ and $G\alpha_q$. Conserved residues are indicated in orange. Residues subjected to point mutations in the chimeric studies are annotated with green dots

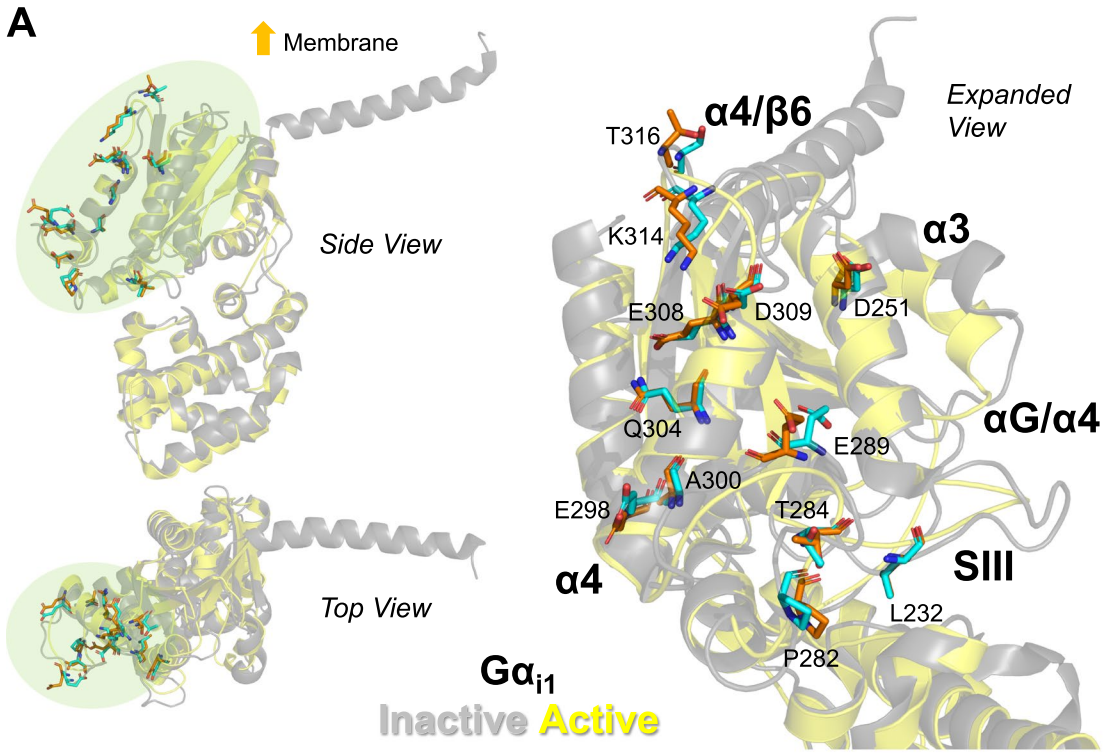

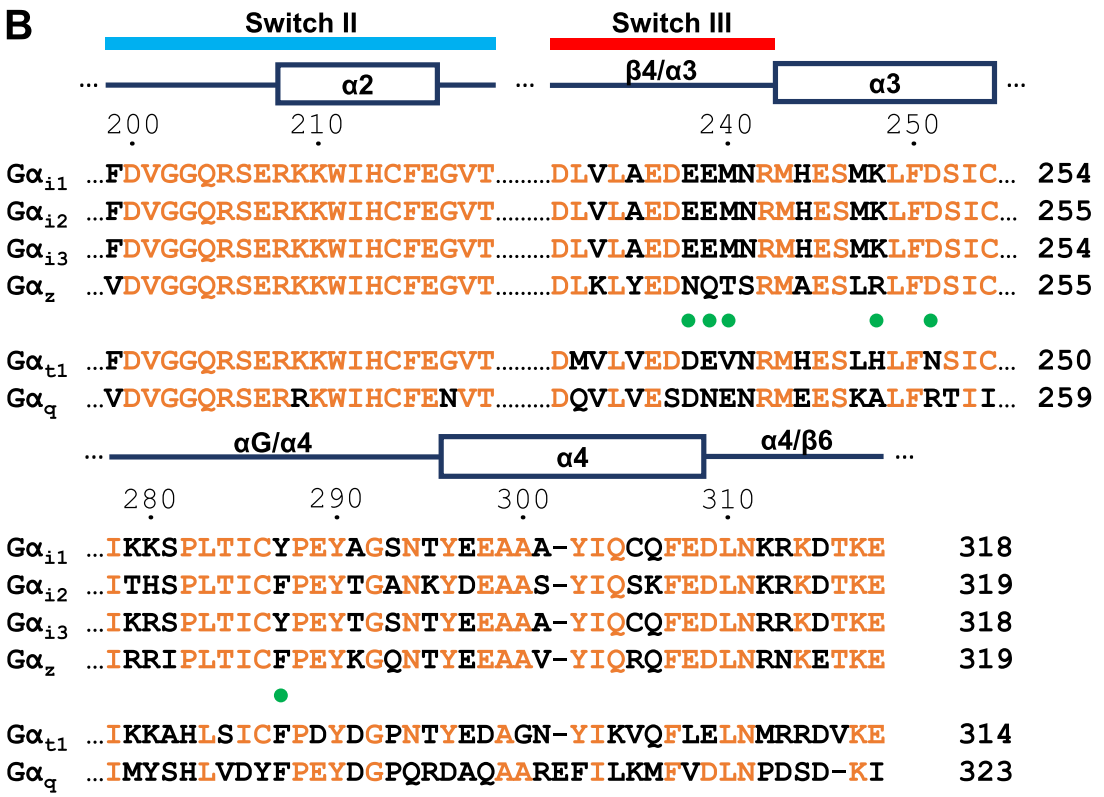

Fig. 1 (See legend on previous page.)

Constitutive activity of $G\alpha_{i1}$RC is abolished by replacement of putative AC-interacting domains of $G\alpha_{i1}$

To test the effects of substitutions/mutations on the function of $G\alpha_{i1}$, chimeras with or without either a QL or RC mutation were transfected into HEK293 cells, followed by the measurement of forskolin-induced [^{3}H] cAMP accumulation. Three chimeric constructs, namely Chi1-KDY, Chi2-KDY and Chi6, showed constitutive stimulation/inhibition of AC activity without the incorporation of QL or RC mutations (Fig. 3A). Both $G\alpha_{i1}$QL and $G\alpha_{i1}$RC mutants suppressed cAMP elevation by forskolin to approximately 60% of the level observed with $G\alpha_{i1}$ (Fig. 3B and C), consistent with previous findings indicating their constitutive activity [34–36]. Interestingly, as compared to the wild-type chimeras, none of the substitutions with $G\alpha_{t1}$ affected the ability of the QL chimeras to inhibit AC (Fig. 3B). Yet, most of the RC chimeras (except Chi4RC) have lost the ability to inhibit cAMP production (Fig. 3C). It is noteworthy that purified Chi2 and Chi4 (referred to as Chi7 and Chi4 respectively in [27]) bind PDEγ as efficiently as an activated $G\alpha_{t1}$ [27], but Chi2QL and Chi4QL/RC remained able to inhibit AC when overexpressed in cells (Fig. 3B). Our findings clearly showed functional differences between $G\alpha_{i1}$QL and $G\alpha_{i1}$RC (albeit both are constitutively active) *in cellulo*. Apparently, the activity of $G\alpha_{i1}$RC can be more easily compromised by chimeric manipulations. A summary of their inhibitory activities towards AC is shown in Table 1.

Chi6 appeared to inhibit AC constitutively (Fig. 3A). As the C-terminus of $G\alpha_q$ is important for effector interaction [33], we sought to test if its effector specificity has been switched to PLCβ which may then indirectly inhibit AC activity [37]. Chi6QL did not stimulate the production of inositol phosphates (IP) whereas constitutively active $G\alpha_q$QL significantly stimulated the PLCβ activity under the same experimental condition (Fig. S1A), suggesting that Chi6 cannot activate PLCβ.

Activity-compromised $G\alpha_{i1}$ chimeras can suppress cAMP level upon receptor activation

In the preceding experiments, many RC-bearing chimeras lost their ability to inhibit AC while most of the chimeric QL mutants remained able to suppress the forskolin response (Fig. 3 and Table 1). The contrasting results obtained with the QL and RC mutants of the chimeras implied that there may be discernable differences in the active conformations promoted by these two mutations. We thus examined which of the two mutants have a closer resemblance to $G\alpha_{i1}$ activated by a receptor, with the latter being more biologically relevant. We determined the chimeras' ability to mediate receptor-induced inhibition of cAMP accumulation. To enable detection of receptor-mediated responses without interference from endogenous G_i proteins, a C351I (CI) mutation was introduced into the chimeras to provide resistance to PTX [38]. Eight chimeras that exhibited differential abilities to abolish the constitutive activities of the QL or RC mutation were selected and their corresponding CI mutants constructed; with the exception of Chi5-CI, these chimeras were expressed at levels comparable to that of the $G\alpha_{i1}$-CI mutant (Fig. 4A). HEK293 cells co-expressing the G_i-coupled dopamine D_2 receptor (D_2R) and a chimera with the CI mutation were pretreated with PTX before assaying for forskolin-induced cAMP accumulation in the absence or presence of 100 nM of quinpirole (agonist for D_2R). PTX treatment effectively inhibited the ability of $G\alpha_{i1}$ to be activated by D_2R (Fig. 4B), hence any detected suppression of cAMP level would be primarily due to the activity of the PTX-resistant chimeras. The positive control, $G\alpha_{i1}$-CI, produced ~ 60% inhibition of forskolin-induced cAMP response upon activation by the receptor (Fig. 4B and C). Surprisingly, all CI chimeras significantly inhibited AC upon D_2R activation (Fig. 4B), albeit weaker than that of $G\alpha_{i1}$-CI (Fig. 4C). The extent of inhibition varied among the chimeras, with a maximum of 50% inhibition observed with Chi3-CI, while Chi1-AAA-CI and Chi5-CI only produced ~ 20% inhibition (Fig. 4C). Chi1-AAA-CI, Chi2-CI and Chi3-CI had an elevated cAMP level upon treatment with forskolin, ranging from a 30% to 50% increase (Fig. 4B).

Because GDP/GTP exchange on the Gα subunit triggered by an activated receptor is initiated from the C-terminal end of the Gα subunit to the switch regions [39], alterations in the C-terminal half of $G\alpha_{i1}$, as in the chimeras, may affect the rate of guanine nucleotide exchange, thereby attenuating its ability to inhibit AC. To test if Chi1, a prototypical chimera, can adopt

(See figure on next page.)

Fig. 2 Construction and expression of $G\alpha_{i1}$ chimeras. **A** Homologous replacements or point mutations on putative effector-interacting domains were made between $G\alpha_{i1}$ (black) and $G\alpha_{t1}$ (orange) (Chi1-4) or $G\alpha_q$ (green) (Chi5 and Chi6). Sites of replacement/mutation are indicated by their residue numbers. The locations of GTPase-deficient mutations, namely R178C and Q204L, and PTX-insensitive mutation (C351I) are highlighted with yellow dots. **B** Expression of the chimeras was verified by Western blotting. HEK293 cells in a 24-well plate were transfected with 0.2 μg of various chimeric constructs and the cell lysates were subjected to immunoblotting using antibodies against $G\alpha_{i1}$ and β-actin. Expressions of the chimeras were compared with that of $G\alpha_{i1}$

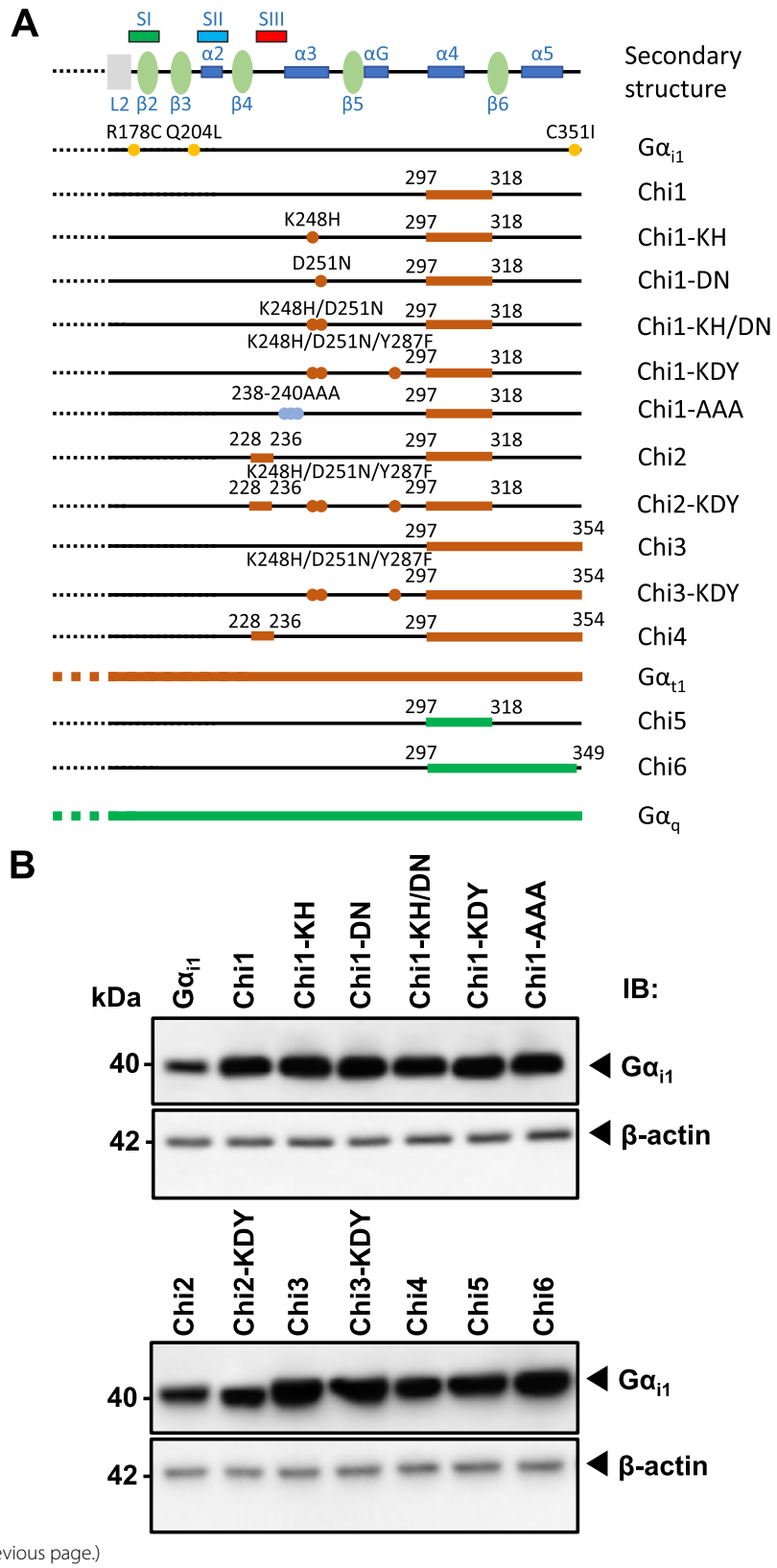

Fig. 2 (See legend on previous page.)

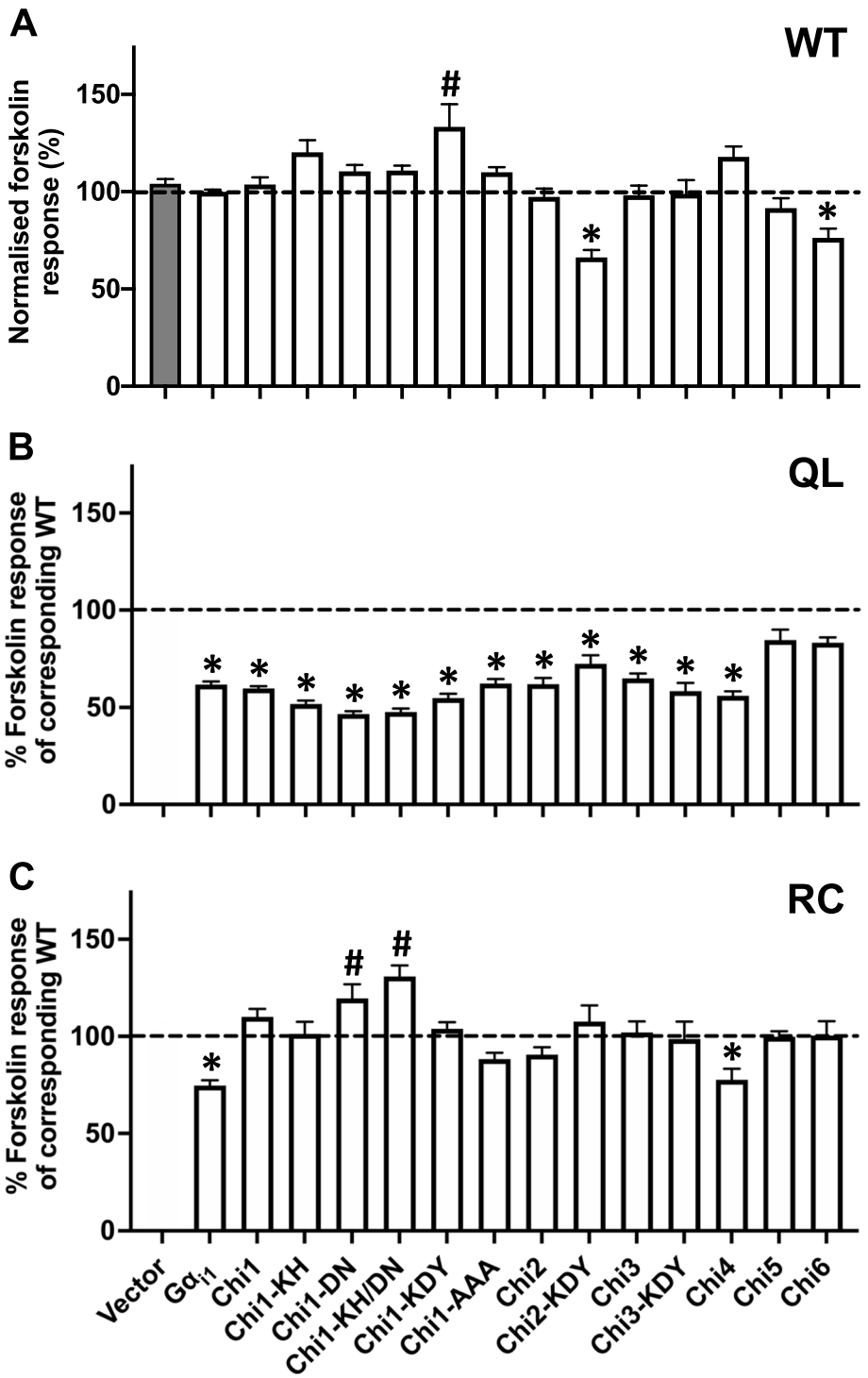

Fig. 3 Effect of the QL/RC-bearing $G\alpha_{i1}$ chimeras on forskolin-induced cAMP accumulation. HEK293 cells were transfected with 0.4 μg/mL of various chimeric constructs, labeled with [^{3}H]adenine, and then assayed for [^{3}H]cAMP accumulation in the presence of 50 μM forskolin. **A** Responses of the chimeras in WT version, as well as cells transfected with empty vector control (gray bar), towards forskolin were normalized against that of $G\alpha_{i1}$. *, significantly lower than $G\alpha_{i1}$; #, significantly higher than $G\alpha_{i1}$. **B**, **C** The relative activities of the QL (**B**) or RC (**C**) chimeras are expressed as a percentage of cAMP accumulation of their corresponding WT. *, significantly lower than the corresponding WT, #, significantly higher than the corresponding WT. Data shown are mean ± SEM ($n = 3$). Bonferroni *t* test, $p < 0.05$

Table 1 Activities of QL-/RC-bearing chimeras towards forskolin response

	cAMP level (% of $G\alpha_{i1}$)		
Gα	**WT**	**QL**	**RC**
$G\alpha_{i1}$	100.0 ± 1.5	57.7 ± 1.5*	70.9 ± 4.9*
Chi1	103.6 ± 3.7	69.0 ± 2.4*	117.9 ± 4.5
Chi1-KH	120.2 ± 6.2	62.2 ± 2.8*	124.8 ± 3.6
Chi1-DN	110.4 ± 3.2	52.5 ± 2.5*	135.0 ± 8.3#
Chi1-KH/DN	110.9 ± 2.4	55.7 ± 2.0*	149.3 ± 7.9#
Chi1-KDY	133.3 ± 11.6†	55.7 ± 2.9*	136.9 ± 8.8#
Chi1-AAA	110.0 ± 2.5	68.5 ± 2.3*	97.1 ± 3.6
Chi2	97.3 ± 4.2	59.6 ± 1.6*	87.6 ± 3.3
Chi2-KDY	66.2 ± 3.9^	47.3 ± 3.8*	67.0 ± 1.8
Chi3	98.2 ± 4.9	63.7 ± 3.4*	98.5 ± 2.4
Chi3-KDY	98.9 ± 7.1	57.7 ± 4.1*	97.4 ± 8.6
Chi4	117.9 ± 5.3	70.3 ± 4.6*	90.9 ± 6.4*
Chi5	91.5 ± 5.0	78.0 ± 6.2	90.8 ± 2.9
Chi6	76.2 ± 4.7^	66.4 ± 3.7	82.2 ± 3.2

HEK293 cells overexpressing the chimeric constructs were subjected to cAMP accumulation assay. Percentage of $G\alpha_{i1}$ was calculated by the fraction of forskolin-stimulated cAMP level in $G\alpha_{i1}$-overexpressing cells. Data are shown as mean ± SEM ($n = 3$). The cAMP levels of QL/RC-bearing chimeras were compared to the chimeras of the wild-type (WT) version. Datum with an asterisk (*) indicates the cAMP level is significantly lower than the WT control, while datum with a hashtag (#) indicates the cAMP level is significantly higher than the WT control. The cAMP levels of chimeras of the WT version were also compared with that of $G\alpha_{i1}$. Datum with (†) indicates an elevated basal cAMP level, while datum with (^) indicates a lower basal cAMP level. Bonferroni *t* test, $p < 0.05$

the active conformation as efficiently as $G\alpha_{i1}$, we examined GTP-induced release of Gβγ in HEK293 cells co-expressing Flag-tagged $G\beta_1$ and HA-tagged $G\gamma_2$ with Chi1 or $G\alpha_{i1}$ (Fig. 4D). Lysates were treated with either aluminum fluoride (AlF_4^-) or GTPγS to activate the Gα subunits. AlF_4^- acts as a mimetic of the γ-phosphate of GTP in GDP•AlF_4^--bound Gα subunits, and it can thus activate Gα subunits without requiring guanine nucleotide exchange (Fig. 4D) [40]. GTPγS is a non-hydrolyzable analog of GTP which locks the Gα subunit into an active conformation upon guanine nucleotide exchange (Fig. 4D) [41]. Activated $G\alpha_{i1}$ should dissociate from the Gβγ dimer and thus would not co-immunoprecipitate with the Flag-tagged $G\beta_1$ subunit (Fig. 4D). Expression of the different G protein subunits in the transfectants was confirmed by Western blots (Fig. 4E). The HA-tagged $G\gamma_2$ was efficiently co-immunoprecipitated with Flag-$G\beta_1$, in line with Gβγ being a constitutive dimer in cells. As shown in Fig. 4F (lanes 5 and 8), both $G\alpha_{i1}$ and Chi1 were pulled down by anti-Flag affinity beads along with the Flag-tagged $G\beta_1$ subunit. Upon treatment with GTPγS, almost all $G\alpha_{i1}$ dissociated from the Gβγ dimer (Fig. 4F, lane 6), but a substantial portion of Chi1 remained associated with the Gβγ dimer (Fig. 4F, lane 9); the extent of co-immunoprecipitation was quantified in Fig. 4G. In contrast, AlF_4^- treatment resulted in the dissociation of ~ 60% of the Gβγ-bound $G\alpha_{i1}$ and Chi1, suggesting that Chi1 can adopt an active conformation similar to $G\alpha_{i1}$ (Fig. 4F and G). Since the effect of GTPγS requires the release of bound GDP from the Gα subunit while the action of AlF_4^- is independent of such an event, these results indicate that the rate of guanine nucleotide exchange of Chi1 may be impaired, leading to apparent reductions in the AC inhibitory activity of the chimeras. This also implies that the loss of activity of RC chimeras is not due to their inability to interact with the downstream effector. Instead, the GTPase deficiency brought about by RC mutation is compromised.

Although Chi5 showed no inhibitory effect on cAMP level (Fig. 3A), Chi5-CI appeared to constitutively inhibit the forskolin-stimulated cAMP accumulation (Fig. 4B), and the forskolin response was further suppressed upon D_2R-induced activation of Chi5-CI (Fig. 4C). Given that Chi5-CI contains the PLCβ-activating domain of $G\alpha_q$ [33], we examined if this chimera could generate IP_3/Ca^{2+} signals via G_q. Quinpirole-induced IP formation was readily observed with $G\alpha_{qz5}$ (positive control) [32] but not with Chi5-CI (Fig. S2A). $G\alpha_{qz5}$ also showed a typical dose–response curve on Ca^{2+} mobilization upon D_2R stimulation, with the maximum signal observed at 100 nM quinpirole (Fig. S2B). Yet, Chi5-CI did not stimulate Ca^{2+} mobilization even at 10 μM quinpirole (Fig. S2B). Therefore, Chi5-CI did not stimulate the G_q signaling pathway.

$G\alpha_{i1}$RC-CI can respond to receptor activation

The ability of D_2R to activate CI-bearing chimeras and suppress the forskolin response (Fig. 4) indicated that these chimeras still contain the necessary domains for interacting with AC. This also explains the inhibitory actions as observed with the chimeric QL mutants (Fig. 3 and Table 1). The lack of constitutive activity of the corresponding RC mutants, however, suggested that the active conformation of these $G\alpha_{i1}$ chimeras cannot be efficiently induced and/or maintained. Hence, we asked if $G\alpha_{i1}$QL and $G\alpha_{i1}$RC would respond differently to receptor activation. The CI mutation was introduced into $G\alpha_{i1}$QL and $G\alpha_{i1}$RC and the resultant mutants, named as $G\alpha_{i1}$QL-CI and $G\alpha_{i1}$RC-CI, were co-expressed with D_2R in HEK293 cells and then subjected to PTX treatment prior to assaying for forskolin-stimulated cAMP accumulation. In the absence of quinpirole, $G\alpha_{i1}$QL-CI significantly suppressed the cAMP level to 50% of that obtained with the control ($G\alpha_{i1}$-CI; Fig. 5A). This constitutive activity of $G\alpha_{i1}$QL-CI was similar to that of $G\alpha_{i1}$-CI-mediated AC inhibition upon D_2R activation by quinpirole, indicating attainment of maximal inhibitory activity. However, cells co-transfected with D_2R and $G\alpha_{i1}$RC-CI produced

an unexpected 20% increase in the forskolin response (Fig. 5A). In the presence of quinpirole, $G\alpha_{i1}$RC-CI significantly inhibited the forskolin response by over 55% (Fig. 5A), thus suggesting that $G\alpha_{i1}$RC-CI can interact with the receptor. This observation is important because it eliminates several possibilities that might account for the loss of AC-inhibitory ability of $G\alpha_{i1}$RC-CI when co-expressed with D_2R. Firstly, as the PTX-insensitive mutants showed similar expression levels (Fig. 5B), the lack of AC inhibition by $G\alpha_{i1}$RC-CI was not attributed to decreased expression of this mutant. Secondly, the ability of quinpirole-treated $G\alpha_{i1}$RC-CI-expressing cells to suppress forskolin-induced cAMP elevation to a level similar to $G\alpha_{i1}$-CI upon receptor activation (Fig. 5A) suggested that $G\alpha_{i1}$RC-CI can adopt an active conformation, allowing its interaction with AC. As Cys-351 is distant from the nucleotide binding pocket of $G\alpha_{i1}$RC [42], it is unlikely that the CI mutation would directly participate in GTP hydrolysis to inactivate $G\alpha_{i1}$RC-CI.

Next, we examined if the loss of activity of RC chimeras is due to their failure to maintain, or alternatively, induce the active conformation of the Gα subunit. To test this, we introduced the CI mutation to Chi1QL and Chi1RC, the prototypical chimeric constructs. Chi1-CI showed approximately 25% suppression of cAMP level upon receptor activation (Fig. 5A). Chi1QL-CI was constitutively active without quinpirole treatment, with the forskolin response reduced to a level similar to an activated Chi1-CI (Fig. 5A). Receptor activation enhanced the inhibition on cAMP level by Chi1QL-CI, suggesting Chi1QL-CI is not fully active (Fig. 5A). Like $G\alpha_{i1}$RC-CI (Fig. 5A), Chi1RC-CI did not inhibit the forskolin-induced cAMP accumulation and showed prominent AC inhibition only upon quinpirole treatment, indicating that the active conformation of Chi1RC-CI is inducible (Fig. 5A). Thus, the loss of AC inhibition by RC chimeras may be attributed to the lack of maintenance of their active conformation.

Chi1RC is RGS-sensitive in cellulo

Since $G\alpha_{i1}$RC-CI and Chi1RC-CI could be activated by D_2R (Fig. 5A), it implies that they may adopt an inactive conformation in the absence of receptor activation despite harboring the RC mutation. Because an active GTP•$G\alpha_{i1}$ has a low affinity for the receptor [43], it further suggests that a substantial portion of the $G\alpha_{i1}$RC-CI is GDP-bound. Given that the RC mutation impairs the intrinsic GTPase activity [44], the GDP-bound state (as opposed to a GTP-locked state) can be obtained by two means: the prevention of GDP/GTP exchange by guanine nucleotide dissociation inhibitors, and the extrinsic promotion of GTP hydrolysis by GTPase-activating proteins (GAPs). An early reconstitution study showed that RGS4 could promote the GTP hydrolysis of $G\alpha_{i1}$RC, but not for $G\alpha_{i1}$QL [24], although *in cellulo* evidence remains lacking. Thus, the lack of constitutive activity of RC chimeras may be attributed to their interaction with RGS proteins which aids in maintaining the GDP-bound state of the Gα subunits. To test this hypothesis, we incorporated an RGS-insensitive G183S mutation [45] into QL/RC-bearing $G\alpha_{i1}$ and Chi1, and then examined their AC inhibitory activities. As shown in Fig. 5C, both QL and RC versions of $G\alpha_{i1}$-G183S constitutively suppressed cAMP accumulation to an extent similar to $G\alpha_{i1}$QL and $G\alpha_{i1}$RC, respectively. It is also worth noting that G183S mutation alone did not produce any effect on AC inhibition (Fig. 5D). These observations suggested that RGS proteins did not hinder the interactions between AC and the two constitutively active mutants. Both Chi1QL and Chi1QL-G183S produced significant AC inhibition (Fig. 5C). Strikingly, G183S mutation enabled Chi1RC to suppress cAMP production (Fig. 5C). Although mutants bearing the G183S mutation showed a lower expression (Fig. 5E), the level was nevertheless sufficient to generate a significant cAMP suppression (Fig. 5C). Collectively, the lack of AC inhibition by Chi1RC, and

(See figure on next page.)

Fig. 4 Activity of PTX-insensitive $G\alpha_{i1}$ chimeras upon receptor activation. HEK293 cells were co-transfected with D_2R and various $G\alpha_{i1}$ constructs (0.2 μg/mL each), treated with PTX (100 ng/mL, 16 h), and then assayed for forskolin-induced [^{3}H]cAMP accumulation in the absence or presence of 100 nM quinpirole. **A** Expression of the PTX-insensitive $G\alpha_{i1}$ chimeric mutants was confirmed by immunoblotting with 20 μg of total protein. **B** Forskolin-stimulated cAMP levels are expressed as a percentage of the response normalized against $G\alpha_{i1}$-CI. **C** Quinpirole-induced activity is expressed as a percentage of inhibition of the forskolin response. Data shown are mean ± SEM ($n = 3$). Bonferroni *t* test, $p < 0.05$; *, significantly lower than the control; #, significantly higher than the control; †, significant inhibition upon receptor activation. **D** Rationale of the subunit dissociation assay. Activated $G\alpha_{i1}$ dissociates with Gβγ, resulting in a drop in $G\alpha_{i1}$ intensity in immunodetection after co-immunoprecipitation with the Flag-tagged Gβ. $G\alpha_{i1}$ activation by GTPγS, but not AlF_4^-, requires guanine nucleotide exchange. **E**–**G** HEK293 cells were transiently co-transfected with 0.2 μg/mL each of Flag-tagged $G\beta_1$, HA-tagged $G\gamma_2$, and either vector (V), $G\alpha_{i1}$ or Chi1. **E** Expressions of the G proteins were confirmed by immunoblotting with 20 μg of the total proteins. **F** 500 μg of the total proteins of the lysate were incubated with or without AlF_4^- (30 μM $AlCl_3$ plus 10 mM NaF) or 100 μM of GTPγS at 37 °C for 15 min prior to immunoprecipitation by anti-Flag affinity gel. **G** Quantification of the co-immunoprecipitation results. Results are expressed as a percentage of $G\alpha_{i1}$ or Chi1 pull-down by Flag-$G\beta_1$. Graph is shown as mean ± SEM ($n = 3$). Student *t* test, $p < 0.05$; †, significantly different

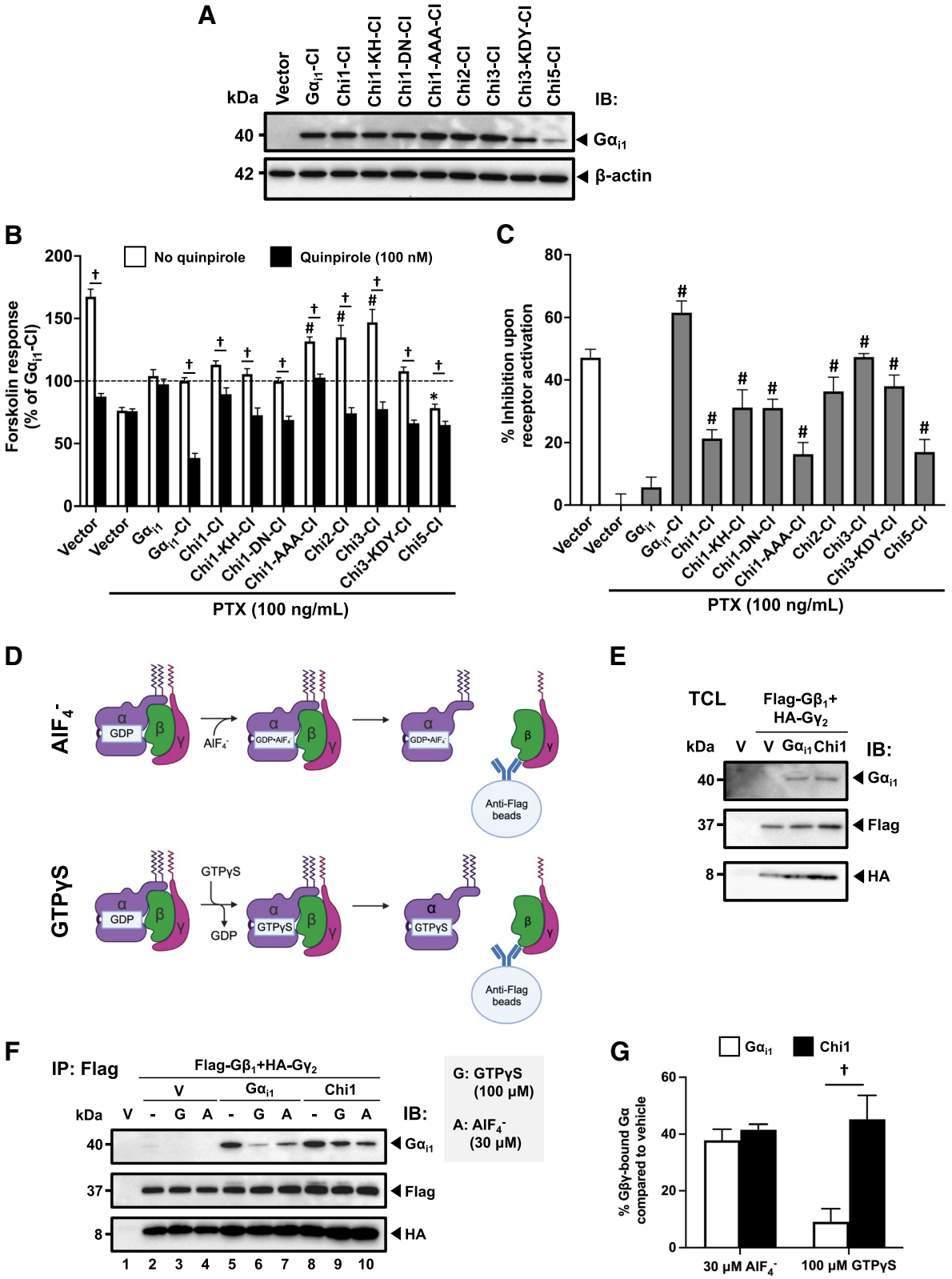

Fig. 4 (See legend on previous page.)

possibly other RC chimeras, might be attributed to 'hyper'-interactions of the Gα subunits with RGS proteins. This also provides the first *in cellulo* evidence that RC mutation is RGS-sensitive.

As Chi1RC-G183S inhibits AC to the same extent as $G\alpha_{i1}$RC (Fig. 5C), one would expect activated Chi1-G183S to dissociate from the Gβγ dimer like a $G\alpha_{i1}$. However, it is also possible that RGS proteins may displace the Gβγ dimer from an active $G\alpha_{i1}$. Co-crystal structures of RGS-$G\alpha_{i1}$ reveal that RGS proteins bind orthogonally to the switch regions of $G\alpha_{i1}$ [25, 46]. In fact, RGS4 inhibited $G\alpha_q$-mediated activation of PLCβ1 by direct blockade of the binding interface [47]. As Gβγ dimer covers the switch regions of $G\alpha_{i1}$ in its inactive, heterotrimeric state [48], RGS proteins may compete with Gβγ dimer for binding $G\alpha_{i1}$. In this case, an activated Chi1-G183S will have a higher association with Gβγ dimer than Chi1, because the G183S mutation prevents Chi1 from binding to RGS proteins [45]. Therefore, we treated lysates of cells expressing Chi1 or Chi1-G183S and $G\beta_1\gamma_2$ with GTPγS and tested for their dissociations with Gβγ dimer. All subunits were well expressed (Fig. 5F). Interestingly, G183S did not affect the extent of dissociation of $G\beta_1\gamma_2$ from either $G\alpha_{i1}$ or Chi1 upon GTPγS treatment (Fig. 5G and H , lanes 5 vs 7 and lanes 9 vs 11). This implies that RGS proteins may form a transient quaternary complex with $G\alpha_{i1}$ and Gβγ dimer to elicit its GAP activity.

$G\alpha_{i1}$ retains its AC inhibitory capability with known switch II mutations

The failure of the chimeras to abolish receptor-induced cAMP suppression (Fig. 4B and C) suggests that there exists an alternative and largely unstudied surface of $G\alpha_{i1}$ which participates in the inhibition of AC. In fact, the α2 helix, which is distally located to the other documented domains (Fig. 6A), was found to be critical for AC interactions of $G\alpha_{i2}$ and $G\alpha_s$ [18]. The α2 helix is part of the switch II region, which has extensive conformational changes upon activation of the Gα subunit (Fig. 6A). In particular, double alanine mutations on K210/I213 of $G\alpha_{i2}$ and the homologous R232/I235 of $G\alpha_s$ (corresponding to K209/I212 of $G\alpha_{i1}$) can eliminate the constitutive activity of their respective RC mutants [18]. Considering the results shown in Figs. 3 and 4, we examined the effect of K209/I212 mutations on $G\alpha_{i1}$. Distinct conformational changes in the side chain orientation of I212, specifically a shifting from a protein-core pointing to an outward pointing configuration during the transition from inactive to active state [42, 48], have been observed, suggesting its potential role in AC interaction. However, the I212A mutant exhibited AC inhibitory activity and did not abrogate the constitutive activity of QL (Fig. 6B). We also substituted I212 with other residues, including leucine (L) and valine (V) to maintain comparable molecular size of the side chain, so that the structural perturbation of the mutations can ideally be minimized. The activity of I212F-QL was also examined, with Phe being the analogous residue in non-AC-interacting $G\alpha_{12/13}$. Interestingly, all I212 substitutions tested failed to suppress the constitutive activity of QL mutation (Fig. 6B) in spite of their comparable expression levels with $G\alpha_{i1}$QL (Fig. 6C). Double K209A/I212A mutation only abolished the activity of RC, but not the QL activity (Fig. 6B). Moreover, cAMP suppressions were still observed from $G\alpha_{i1\text{-}i3}$-CI bearing the double mutations upon activation by D_2R (Fig. 6D). This is consistent with our observations that chimeras which failed to abolish the constitutive activity of QL remained activatable by receptors (Fig. 4). This also supports our notion that RC may not be the best representative of an activated $G\alpha_i$, because a loss of constitutive activity of RC was similarly observed with $G\alpha_{i2}$ bearing the cognate mutations ($G\alpha_{i2}$K210A/I213A-RC; [18]).

(See figure on next page.)

Fig. 5 RC mutants can be activated by receptor and suppressed by RGS. **A** HEK293 cells were co-transfected with D_2R and various $G\alpha_{i1}$-CI or Chi1-CI mutants and assayed similarly to Fig. 4B. The forskolin-stimulated cAMP levels of the chimeras with a CI mutation are expressed as a percentage of the response obtained with $G\alpha_{i1}$-CI. Data shown are mean ± SEM ($n = 3$). Bonferroni *t* test, $p < 0.05$; *, significantly lower than the control; #, significantly higher than the control; †, significant inhibition upon receptor activation. **B** Expression of the PTX-insensitive mutants was confirmed by immunoblotting with 20 μg of total protein. **C**-**E** HEK293 cells were transfected with QL-bearing $G\alpha_{i1}$ constructs and assayed similarly to Fig. 3. **C** Relative activities of the constitutively active chimeras are expressed as a percentage of cAMP accumulation of their corresponding WT. *, significantly lower than the corresponding WT; #, significantly higher than the corresponding WT. Data shown are mean ± SEM ($n = 3$). Bonferroni *t* test, $p < 0.05$. **D** Responses of the chimeras in WT version towards forskolin were normalized against that of $G\alpha_{i1}$. **E** Expression of $G\alpha_{i1}$ constructs were confirmed by immunoblotting with 20 μg of total protein. **F**–**H** HEK293 cells were transiently co-transfected with Flag-$G\beta_1$, HA-$G\gamma_2$, and with or without various $G\alpha_{i1}$ constructs and assayed by subunit dissociation assay as in Fig. 4D. **F** Expressions of the G proteins were confirmed by immunoblotting with 20 μg of the total proteins. **G** 500 μg of the total proteins of the lysate were incubated with or without 100 μM of GTPγS at 37 °C for 15 min prior to immunoprecipitation by anti-Flag affinity gel. **H** Quantification of the co-immunoprecipitation results. Results are expressed as a percentage of the corresponding $G\alpha_{i1}$ or Chi1 constructs pull-down by Flag-$G\beta_1$. Graph shown as mean ± SEM ($n = 3$). Student *t* test, $p < 0.05$; n.d., not detectable; ns, non-significant; #, significantly higher than the control

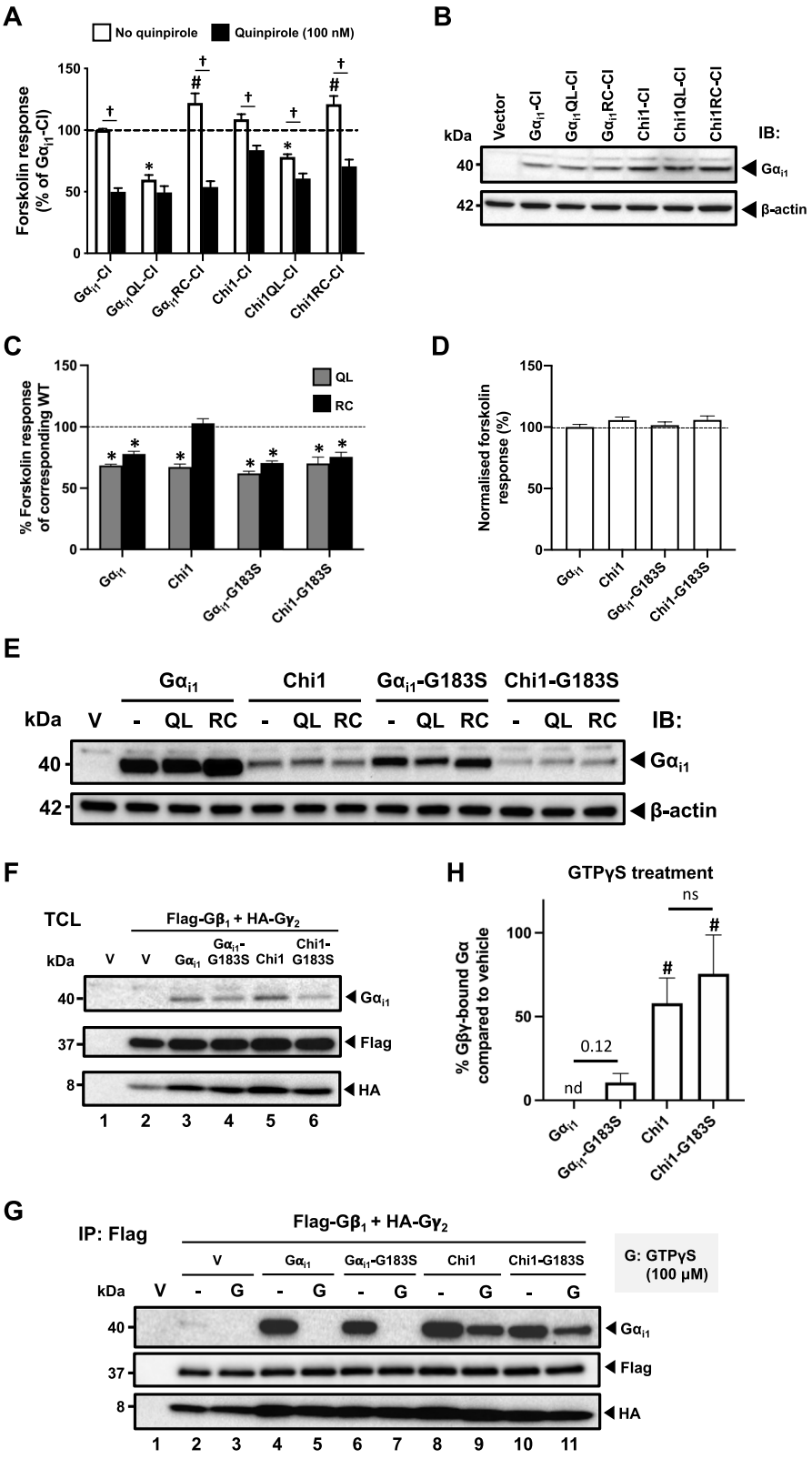

Fig. 5 (See legend on previous page.)

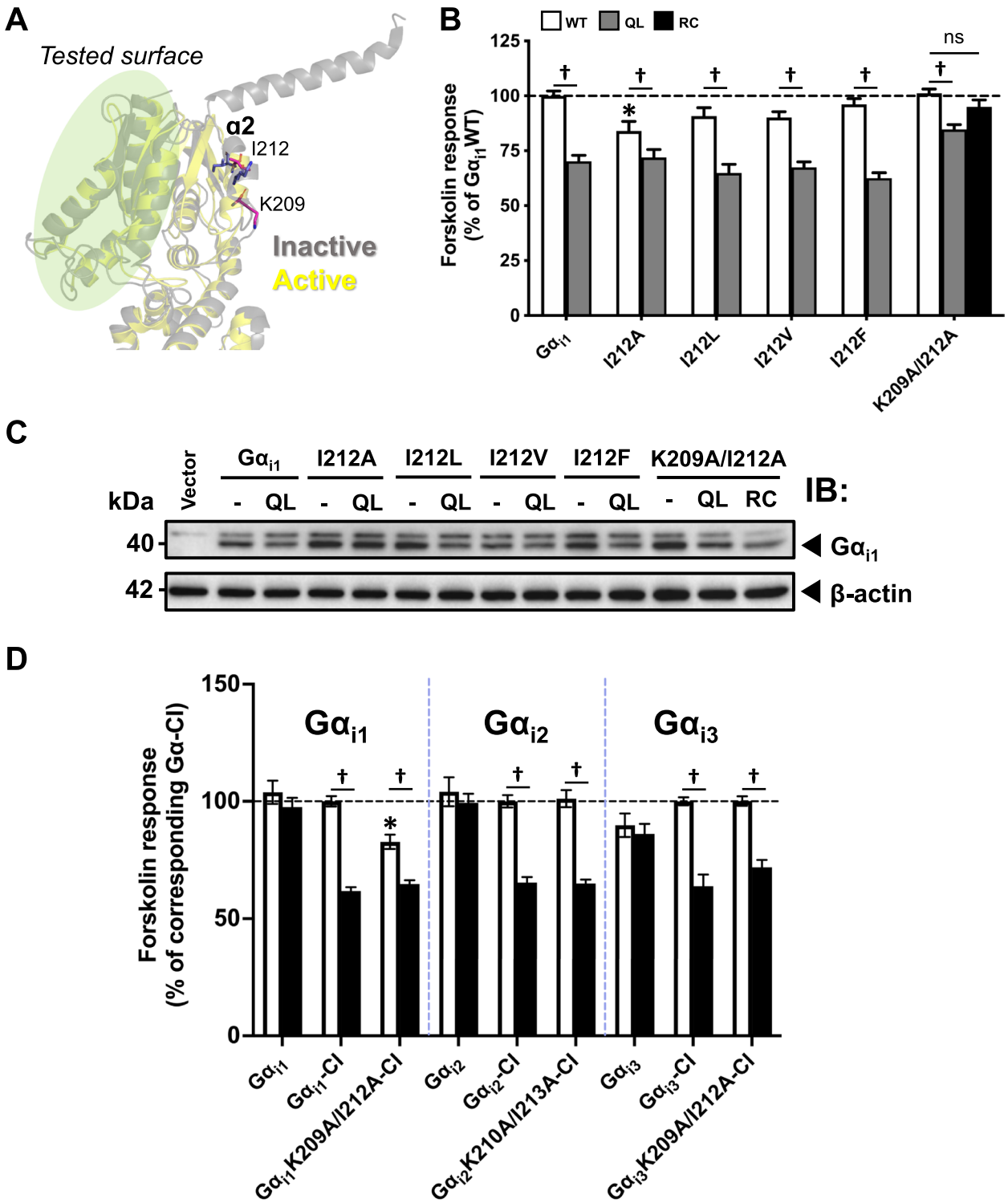

Fig. 6 Effect of K209 and I212 mutations on the AC inhibition QL/RC. **A** Expanded view of the 3-dimensional structure of $G\alpha_{i1}$ highlighting the tested surface (in light green) and the location of K209 and I212 (in sticks) at the α2 helix. **B** HEK293 cells were transfected with various QL/RC-bearing $G\alpha_{i1}$ constructs and assayed similarly to Fig. 3. The relative activities of the constitutively active chimeras are expressed as a percentage of cAMP accumulation of $G\alpha_{i1}$. Data shown are mean ± SEM ($n = 3$). Bonferroni *t* test, $p < 0.05$; ns, non-significant; †, significant inhibition. **C** Expression of $G\alpha_{i1}$ constructs were confirmed by immunoblotting with 20 μg of total protein. **D** HEK293 cells were co-transfected with D_2R and various $G\alpha_{i1-3}$ mutants and assayed as in Fig. 4B. The forskolin-stimulated cAMP levels of the chimeras with a CI mutation are expressed as a percentage of the response normalized with the corresponding Gα-CI. Data shown are mean ± SEM ($n = 3$). Bonferroni *t* test, $p < 0.05$; *, significantly lower than the control; †, significant inhibition upon receptor activation

$G\alpha_{i1}$QL remains constitutively active with mutations that target potential AC-interacting residues

We have also investigated other potentially novel sites for interaction with AC (Fig. S3). The proximity of positively charged residues in $G\alpha_{i1}$ near switch II (K35, H188, and K197) suggests their potential to form charge-charge interactions with AC5/AC6. Additionally, the E489 residue located in the C1 domain of the AC5 protein (Uniprot: O95622-1), known for its role in $G\alpha_i$-mediated AC inhibition [49], holds promise for forming specific charge-charge interactions with these residues within $G\alpha_{i1}$. Similarly, E216 and K257 in $G\alpha_{i1}$ may play a role in the interaction with AC in view of known interactions between the homologous N239 and R280 in $G\alpha_s$ and the AC9 protein [50]. We generated a double alanine mutant (E216A/K257A) and an E216K/K257E mutant to explore the significance of the charge interactions between these two residues of $G\alpha_{i1}$ and AC. Previous research revealed that mutation in the αG-α4 loop significantly impacts the stimulatory activity of the $G\alpha_s$, despite its spatial distance from the switch II [21]. This suggests that the corresponding loop in the $G\alpha_{i1}$, akin to $G\alpha_s$, may interact with AC. To explore this further, we substituted residues PLT (282–284) in the αG-α4 loop of $G\alpha_{i1}$ with the HLS residues from $G\alpha_{t1}$, creating the mutant termed PLT. These mutants were evaluated for the possible loss of AC inhibition function (Fig. S3). However, all QL-bearing mutants with additional mutations at the described residues remained capable of suppressing forskolin-induced cAMP accumulation (Fig. S3), reflecting that these residues/regions are not critical to AC interaction by $G\alpha_{i1}$.

Additional mutations on the α3/β5 loop synergistically abolished receptor-induced AC inhibition of $G\alpha_{i1\text{-}i3}$ with the α4/β6 loop

Although point mutations on the α2 helix of $G\alpha_{i1}$ failed to entirely eliminate the ability of $G\alpha_{i1}$ to inhibit AC (Fig. 6), it remains possible that adjacent regions may participate in effector recognition. The α2 helix is almost completely covered by Gβ subunit in the GDP-bound inactive state [48], and it undergoes extensive conformational changes upon GTP binding [42]. The subsequent Gβγ release exposes surfaces encompassing the α2 helix. Thus, it is likely that the surrounding residues could be important for effector recognition.

The challenge of our investigation lies in the lack of a crystal structure of the $G\alpha_{i1}$-AC complex. To circumvent this limitation, we employed High Ambiguity Driven protein – protein DOCKing (HADDOCK) to simulate the interactions between a well-resolved structure of an active $G\alpha_{i1}$ and the AlphaFold-simulated structures of human AC5 and AC6, the two AC subtypes known to interact with $G\alpha_{i1}$ [51, 52]. K208, K209, and I212 of $G\alpha_{i1}$ were previously designated as "active" residues in interacting with ACs [18]. For AC5, we selected E489, M492, T493, L550, and V554 of the C1 domain (and E399, M402, T403, L460, and V464 for AC6) as "active" residues [49]. The simulations resulted in 174 predicted $G\alpha_{i1}$-AC5 structures into 5 clusters based on similarity between individual models, representing 87% of the water-refined models (Table 2). Similarly, for the $G\alpha_{i1}$-AC6 complex, HADDOCK predicted 139 structures in 9 clusters, constituting 69% of the generated models (Table 2). Given

Table 2 Parametric data on HADDOCK 2.4 predictions of $G\alpha_{i1}$ and AC5/AC6 interactions

	HADDOCK score	Cluster size	RMSD	Van der Waals energy	Electrostatic energy	Desolvation energy	Restraints violation energy	Buried surface area	Z-score
$G\alpha_{i1}$-AC5									
Cluster 1	-94.8 ± 2.5	84	19.4 ± 0.1	35.2 ± 5.6	-225.0 ± 29.5	-14.8 ± 2.5	2.0 ± 1.7	1367.6 ± 113.0	-0.9
Cluster 2	-93.7 ± 6.6	42	17.2 ± 0.2	-27.4 ± 4.1	-284.8 ± 17.7	-10.1 ± 3.8	7.1 ± 2.2	1433.4 ± 69.9	-0.8
Cluster 4	-88.0 ± 1.4	17	18.6 ± 0.2	-40.5 ± 2.1	-153.8 ± 24.0	-17.0 ± 4.2	3.0 ± 1.1	1287.7 ± 25.6	-0.2
Cluster 3	-84.7 ± 0.7	23	12.5 ± 0.2	-41.0 ± 4.6	-183.6 ± 41.4	-8.1 ± 3.9	11.7 ± 6.6	1537.2 ± 50.6	0.1
Cluster 5	-67.5 ± 7.8	8	1.2 ± 0.2	-23.6 ± 2.6	-217.2 ± 35.0	-2.5 ± 3.2	19.9 ± 18.9	1294.9 ± 59.1	1.9
$G\alpha_{i1}$-AC6									
Cluster 1	-100.5 ± 9.8	70	1.6 ± 1.0	-42.0 ± 6.7	-234.4 ± 41.7	-13.5 ± 2.0	19.1 ± 16.7	1476.7 ± 91.4	-1.9
Cluster 2	-85.6 ± 4.6	21	17.8 ± 0.2	-45.5 ± 2.1	-208.8 ± 17.7	-0.6 ± 1.3	22.5 ± 19.1	1709.5 ± 60.7	-1.0
Cluster 3	-79.1 ± 4.1	12	9.3 ± 0.3	-37.5 ± 3.9	-242.3 ± 41.4	6.5 ± 2.1	3.6 ± 1.7	1333.6 ± 39.9	-0.7
Cluster 4	-68.6 ± 4.0	11	6.4 ± 1.1	-33.0 ± 4.4	-163.2 ± 33.9	-5.2 ± 3.5	22.5 ± 32.9	1184.0 ± 108.8	-0.1
Cluster 6	-64.3 ± 6.7	6	10.4 ± 0.3	-19.8 ± 2.1	-267.8 ± 35.5	6.7 ± 2.6	23.5 ± 10.5	1250.8 ± 119.6	0.1
Cluster 9	-57.6 ± 12.1	4	3.1 ± 0.2	-23.9 ± 4.8	-162.0 ± 34.5	-1.4 ± 1.7	2.0 ± 0.8	1212.2 ± 228.0	0.5
Cluster 7	-55.6 ± 6.1	5	5.6 ± 1.7	-28.1 ± 3.8	-166.0 ± 31.9	3.4 ± 3.0	22.8 ± 13.3	1166.9 ± 131.2	0.6
Cluster 5	-51.4 ± 9.1	6	14.8 ± 0.3	-25.8 ± 5.1	-106.6 ± 39.8	-5.3 ± 4.5	9.7 ± 12.7	1171.7 ± 107.0	0.8
Cluster 8	-37.3 ± 7.1	4	12.4 ± 0.1	-14.1 ± 5.0	-77.7 ± 22.1	-8.6 ± 3.5	9.0 ± 1.6	789.9 ± 123.1	1.6

the higher reliability attributed to the top cluster with the lowest Z-score, we focused on investigating the structures from the leading cluster in each simulation.

The only crystal structure available for AC in complex with a Gα subunit is that of $G\alpha_s$-AC9 [50]. Despite AC9 being unresponsive to inhibition by $G\alpha_i$ [53], we utilized it as a benchmark to assess the reliability of structural predictions by HADDOCK. The predicted co-complexes of $G\alpha_{i1}$-AC5 and $G\alpha_{i1}$-AC6 generally exhibited a binding pattern reminiscent of the $G\alpha_s$-AC9 structure (Fig. 7A and B). We observed a key interaction interface where the α2 helix of $G\alpha_{i1}$ inserts into the groove formed by the α2 and α3 helices of the C1 domains of AC5 and AC6 (Fig. 7C and D), akin to the α2 helix of $G\alpha_s$ interacting with the C2 domains of AC9. Similar binding modes were also evident in other top clusters, specifically clusters 2 and 4 for $G\alpha_{i1}$-AC5, and clusters 4 and 9 for $G\alpha_{i1}$-AC6 (data not shown). Subsequently, we analyzed the molecular interactions within the binding interfaces using PRODIGY and PDBsum. We identified 45 interactions between $G\alpha_{i1}$ and AC5 and 58 interactions with AC6, which are comparable to $G\alpha_s$-AC9 where 64 interactions were observed (Table 3). In the $G\alpha_{i1}$-AC5 complex, interacting residues were clustered in several domains, including the α2 helix (R208-H213), the α2/β4 loop (F215-E216), the α3 helix (S252), and the α3/β5 loop (N255-W258) (Fig. S4). It was similarly observed for $G\alpha_{i1}$-AC6, where the α2 helix (R205, R208-H213), the α2/β4 loop (F215), the α3 helix (L249, S252-I253), the α3/β5 loop (N256-W258), and the α4/β6 loop (D315-T316) were identified as sites of interaction (Fig. S4). These predictions are aligned with another molecular dynamic simulation study [54]. Notably, the α3/β5 loop is the only predicted region that was not previously studied. The predicted models indicated that the α3/β5 loop is coplanar to the α2 helix of $G\alpha_{i1}$, and interacts with both AC5 and AC6 by forming multiple polar and apolar attractions with the key residues of the C1 domain (Figs. 7C, D and S4). Moreover, the α3/β5 loop is highly conserved in AC-inhibiting $G\alpha_{i1\text{-}3/z}$ (Fig. 7E).

Consequently, we examined whether the replacement of N255-F259 of $G\alpha_{i1}$ (NNKWF) with that of $G\alpha_{t1}$ (NHRYF), named NKW (Fig. 7E), could potentially impact its ability to effectively recognize AC. NKW showed a slight activation towards AC and its QL version showed diminished constitutive activity (15.6 ± 1.6% in NKW-QL versus 35.4 ± 2.5% in $G\alpha_{i1}$QL; Fig. 8A). Strikingly, the cAMP suppression contributed by the QL point mutation was abolished by a chimera combining NKW with Chi1 mutation (named Chi1-NKW-QL, -9.6 ± 4.5% inhibition) (Fig. 8A). Such observation may not be owing to the lower expression level of Chi1-NKW than $G\alpha_{i1}$ and Chi1 (Fig. 8B and D), as even lesser expressions of QL/RC-bearing mutants (as seen in the case of Chi1-G183S) were adequate to inhibit AC activity (Fig. 5C and E). Moreover, NKW maintained a normal GDP/GTP exchange rate similar to the wild-type, while both Chi1 and Chi1-NKW showed a similar defect in this process (Fig. 8C and E).

We then tested if these mutants can respond to receptor activation. NKW-CI suppressed forskolin-induced cAMP elevation when D_2R was activated, in line with our observations on other QL-bearing chimeras (Fig. 8F and G). Remarkably, Chi1-NKW-CI lost the ability to inhibit cAMP upon quinpirole treatment (Figs. 8F and G). Cognate mutations were also found to eliminate the activity of $G\alpha_{i2}$ and $G\alpha_{i3}$ upon receptor activation (Fig. 8F and G); the mutants were expressed in levels similar to their respective Gα (Fig. 8H). These results indicated that the α3/β5 loop, the α4 helix, and the α4/β6 loop cooperatively mediate the AC inhibition by $G\alpha_{i1\text{-}3}$. They also shed light on the mechanism through which different Gα members within the same family distinguish effectors. Notably, the α3/β5 loop, the α4 helix, and the α4/β6 loop might play a pivotal role in preventing $G\alpha_{t1}$ from inhibiting AC.

Discussion

The regulation of AC activity by G proteins has long been recognized as a major signaling event which controls numerous cellular processes, but the precise mechanism remains poorly defined. Available biochemical evidence suggests that the opposing effects of $G\alpha_s$ and $G\alpha_i$ subunits are not due to competition for AC, since they apparently bind to different domains of the effector [49]. Recent advances in structural elucidation techniques have provided a detailed understanding on how $G\alpha_s$ interacts with type 9 adenylyl cyclase [50]. However, far less is known pertaining to how $G\alpha_i$ subunits inhibit AC. Given that the four AC-inhibiting $G\alpha_i$ subunits are highly homologous, one might expect that previous experimental

(See figure on next page.)

Fig. 7 HADDOCK predictions on $G\alpha_{i1}$-AC interactions. Three-dimensional structures on the best-scored predicted models showing **A** $G\alpha_{i1}$-AC5 (in light blue and pink, respectively) and **B** $G\alpha_{i1}$-AC6 (in wheat and green, respectively) interactions. Expanded views showing the interfaces of binding between $G\alpha_{i1}$ and AC5 or AC6 were shown in (**C**) and (**D**) respectively. Locations of the key residues on the α3/β5 loop predicted to be important for such interactions are shown in sticks. **E** Sequence alignment of the region spanning the α3 helix to the β5 sheet of AC-inhibiting Gα, and $G\alpha_{t1}$. Conserved residues are indicated in orange

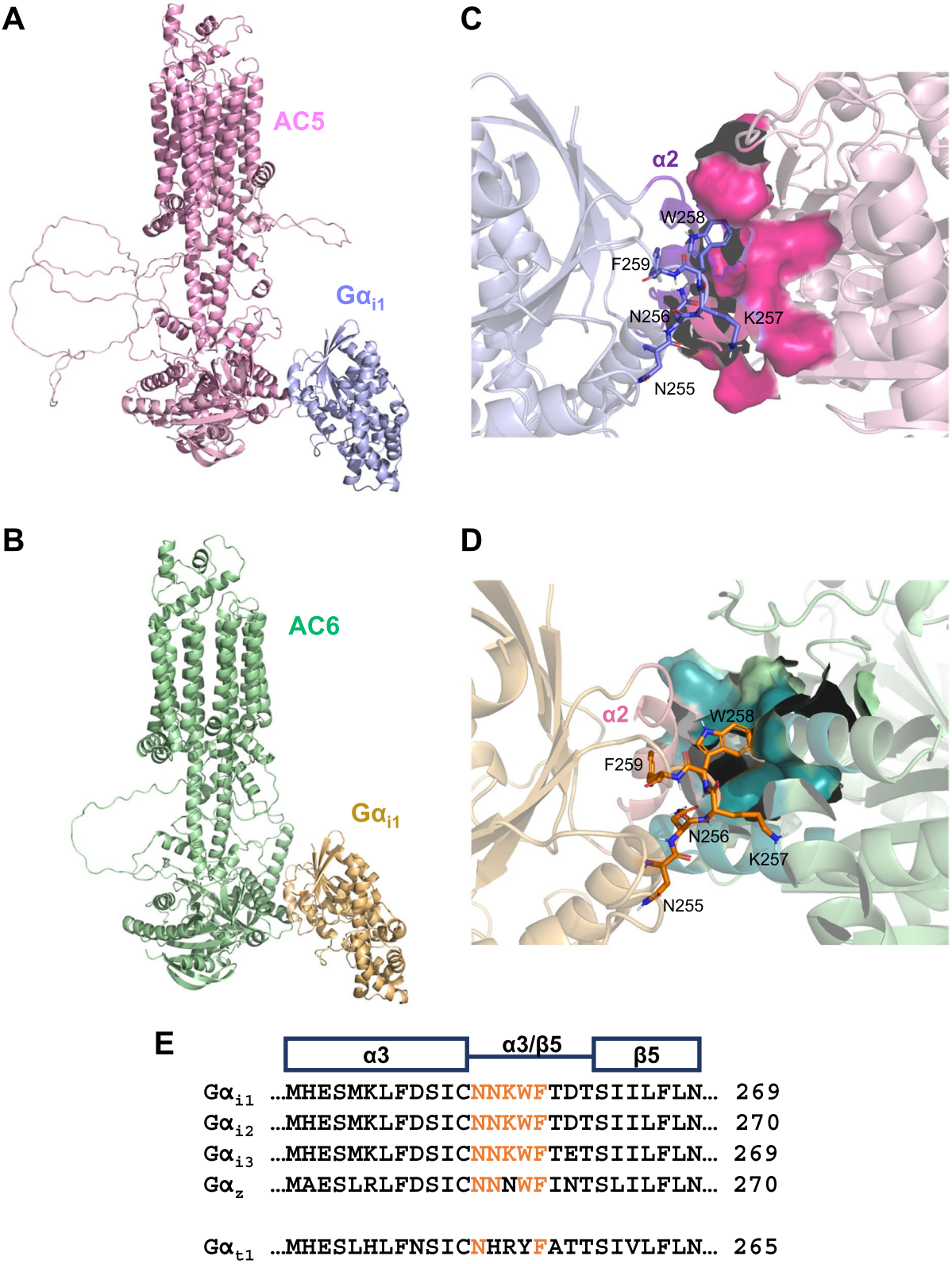

Fig. 7 (See legend on previous page.)

Table 3 PRODIGY predictions of intermolecular forces between Gα and AC isoforms

Complex	ΔG (kcal mol^{-1})	Kd(μM) at 37℃	Charged-charged interactions	Charged-polar interactions	Charged-apolar interactions	Polar-polar interactions	Polar-apolar interactions	Apolar-apolar interactions	Total no. of Interactions
$G\alpha_{i1}$-AC5	-6.9	14.0	6	11	9	1	7	11	45
$G\alpha_{i1}$-AC6	-8.6	0.93	9	11	20	1	8	9	58
$G\alpha_{s}$-AC9	-9.3	0.29	6	7	17	2	14	18	64

findings on $G\alpha_{i2}$ and $G\alpha_{z}$ [17–19] will be applicable to $G\alpha_{i1}$, and thus allow a more precise mapping of AC-interacting residues against the $G\alpha_{i1}$ crystal structures. The present study, however, suggests otherwise since substitution of putative AC-interacting domains in the chimeras failed to abolish inhibitory regulation on AC by the G_i-coupled D_2R (Fig. 4). We further identified a tripeptidic motif (NKW) in the α3/β5 loop as an additional region required for AC inhibition by $G\alpha_{i1-3}$ (Fig. 8). This domain has been overlooked in early mapping studies, because it was assumed that the constitutively active mutants of $G\alpha_i$, a tool commonly used in those studies [17–19], functionally mirrored that of a receptor-activated $G\alpha_i$. Our results clearly suggested that, however, QL and RC do not resemble a receptor-activated $G\alpha_i$. Firstly, chimeras that replaced putative AC-interacting domains of $G\alpha_{i1}$ with distantly related Gα subunits could only abolish the constitutive activity arising from the RC mutation (Fig. 3). Secondly, $G\alpha_{i1}$RC-CI, but not $G\alpha_{i1}$QL-CI can be activated by receptors (Fig. 5A). Thirdly, RC mutation, but not QL mutation, is RGS-sensitive (Fig. 5C). Although both QL and RC mutations impede GTP hydrolysis and result in constitutive activation of the Gα subunits, it appears that $G\alpha_{i1}$QL is functionally more similar to a receptor-activated $G\alpha_{i1}$ in a cellular environment. As both Gln204 and Arg178 are conserved among all Gα subunits, the choice of using QL or RC mutants to demonstrate constitutive Gα activity should be carefully considered.

It is interesting to note that the present observations generally agree with previous reports [22–24], wherein the constitutive activity of the RC mutants are more prone to disruptions than the QL mutants (Fig. 3). Coleman et al. have previously compared the X-ray crystal structures of $G\alpha_{i1}$ bound by GTPγS and GDP-AlF_4^- respectively [42]. The slight changes in the shape of the nucleotide-binding pocket between the two crystal structures insinuated different roles of Gln204 and Arg178 in GTP hydrolysis. The glutamine residue orients a water molecule towards the γ-phosphate of GTP to initiate a nucleophilic attack, whereas the arginine residue stabilises the GDP-P_i transition state [42]. Thus, one may expect that the thermodynamic requirement for GTP hydrolysis could be more easily overcome in RC mutation than in QL mutation, because the latter mutation would completely abolish the initiation condition for the reaction.

The observation that $G\alpha_{i1}$RC-CI suppresses AC only with receptor activation suggested that a substantial population of the molecule remains GDP-bound (Fig. 5A). This is in line with an early study on purified $G\alpha_{i1}$RC and $G\alpha_{i1}$QL, wherein only ~ 40% of $G\alpha_{i1}$RC (as compared with 100% for $G\alpha_{i1}$QL) were GTP-bound in steady-state, despite being equally GTPase-deficient [36]. Another study observed that only purified $G\alpha_{i1}$RC, but not $G\alpha_{i1}$QL, was sensitive to AlF_4^- (a mimetic of the γ-phosphate of GTP in GDP•AlF_4^--bound Gα subunits), implying that there exists a subpopulation of GDP-bound $G\alpha_{i1}$RC [42]. In fact, an in vitro study on $G\alpha_{s}$RC

(See figure on next page.)

Fig. 8 Cooperation between the α3/β5 loop, the α4 helix and the α4/β6 loop in activating AC-inhibiting Gα. For panels A and B, HEK293 cells were transfected with various QL-bearing $G\alpha_{i1}$ constructs and assayed similarly to Fig. 3. For panels C to E, HEK293 cells were co-transfected with D_2R and various $G\alpha_{i1-3}$ mutants and assayed similarly to Fig. 4B. **A** The relative activities of the constitutively active chimeras are expressed as a percentage of cAMP accumulation of $G\alpha_{i1}$. Data shown are mean ± SEM ($n = 3$). Bonferroni *t* test, $p < 0.05$; #, significant increase relative to control; ns, not significant; †, significant inhibition. **B**,**H** Expression of $G\alpha_{i1}$ constructs were confirmed by immunoblotting with 20 μg of total protein. For panels C and D, HEK293 cells were transiently co-transfected with Flag-$G\beta_1$, HA-$G\gamma_2$, with or without various $G\alpha_{i1}$ and assayed by subunit dissociation assay as in Fig. 4D. **C** 500 μg of the total proteins of the lysate were incubated with or without 100 μM of GTPγS at 37 °C for 15 min prior to immunoprecipitation by anti-Flag affinity gel. **D** Expressions of the G proteins were confirmed by immunoblotting with 20 μg of the total proteins. **E** Quantification of the co-immunoprecipitation results. Results are expressed as a percentage of the corresponding $G\alpha_{i1}$ constructs pull-down by Flag-$G\beta_1$. Graph is shown as mean ± SEM (n ≥ 3). Student *t* test, $p < 0.05$; ns, non-significant; #, significantly higher than the control. **F** The forskolin-stimulated cAMP levels of the chimeras with a CI mutation are expressed as a percentage of the response normalized with the corresponding Gα-CI. **G** The forskolin response in the presence of quinpirole is expressed as a percentage inhibition of the fraction of cAMP level upon quinpirole stimulation. Data shown are mean ± SEM ($n = 3$). Bonferroni *t* test, $p < 0.05$; ns, non-significant; *, significantly lower than the control; #, significantly higher than the control; †, significant inhibition upon receptor activation

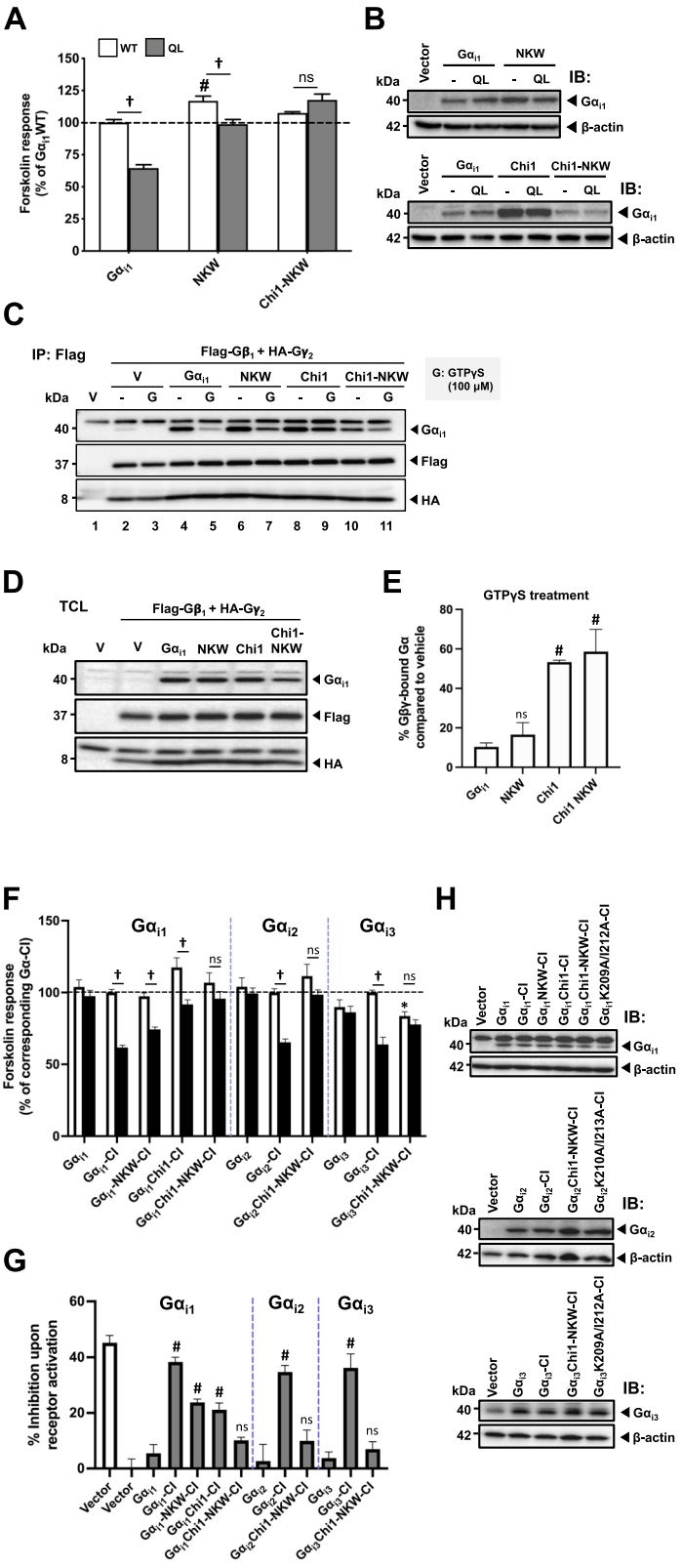

Fig. 8 (See legend on previous page.)

(R204C) also suggested that only around one-third of the expressed mutant was GTP-bound [55]. The conformation of purified GDP-bound $G\alpha_s$RC resembles that of an active, GTPγS-bound $G\alpha_s$ by stabilizing intramolecular hydrogen bonds. Furthermore, GDP-bound $G\alpha_s$RC can bind to the catalytic domain of AC and elevate cellular cAMP level in vitro [55]. Yet, despite the strict conservation of this arginine residue in all Gα subunits, the conformation of GDP-bound $G\alpha_{i1}$RC might not resemble an active $G\alpha_{i1}$ at all. This postulation was supported by our observation that $G\alpha_{i1}$RC-CI only exhibited inhibitory actions on AC upon receptor activation (Fig. 5A). This implies that $G\alpha_{i1}$RC does not seem to stably adopt an active conformation. Alternatively, GDP-bound $G\alpha_{i1}$RC may be forced to adopt an inactive conformation when it is pre-coupled to the receptor. This may explain why $G\alpha_{i1}$RC constitutively inhibits AC when expressed alone, but lost its activity upon co-expression with D_2R (Figs. 3C and 5A). The responsiveness of the RC mutants to receptor stimulation raises the possibility that active RC mutants may accumulate over time due to stimulation by endogenous receptors, which would depend on the rate of generation of GTP-bound RC mutants and their turnover rate or half-life.

Sensitivity of $G\alpha_{i1}$RC towards RGS has been documented in an early reconstitution study [24]. RGS proteins are believed to replace the role of the arginine residue in stabilising the transition state during GTP hydrolysis [25]. The aid of RGS proteins is exceptionally important for members of the $G\alpha_{i/o}$, such as RGS20/$G\alpha_z$, and members of the R4 family/$G\alpha_{i1\text{-}3,oA,oB}$ [56, 57]. Structural studies revealed that RGS proteins directly bind to the switch region of an activated Gα subunits and stabilise the residues for GTP hydrolysis [25, 46]. Time-resolved Fourier Transform Infrared microscopy and molecular dynamic simulation suggested that Arg-178 of $G\alpha_{i1}$ interacts additionally with the α-phosphate of GTP in the presence of RGS4, hence catalysing the leaving of γ-phosphate by eclipsing all three phosphate groups of GTP, while the thermodynamic profile of Gln-204 was unaffected by RGS4 [58]. Herein, we provide the first *in cellulo* evidence that the activity of $G\alpha_{i1}$RC can be turned off by RGS proteins. Chi1RC failed to suppress forskolin-mediated cAMP accumulation, but its inhibitory activity was rescued by an additional G183S mutation, which abolishes the binding of RGS proteins (Fig. 5C). This cannot be explained by potential alteration in the conformation of Gα subunit, because Chi1RC-G183S showed a similar extent of AC inhibition with $G\alpha_{i1}$RC (Fig. 5C). The ability of $G\alpha_{i1}$RC, but not $G\alpha_{i1}$QL, to interact with RGS proteins implies that $G\alpha_{i1}$RC is mainly at a GDP•P_i transition state of GTP hydrolysis in the cells, because RGS4 can only bind to GDP•AlF_4^--complexed $G\alpha_{i1}$, but not to $G\alpha_{i1}$ loaded with non-hydrolysable GTPγS [59]. This further supports our postulation that a substantial fraction of cellularly expressed $G\alpha_{i1}$RC is GDP-bound, which is in line with the previous reconstitution study [36]. The restoration of GTP hydrolysis of $G\alpha_{i1}$RC upon RGS4 co-treatment [24], as well as our observation that Chi1RC regained AC inhibitory action with RGS uncoupling (Fig. 5C), tend to suggest a direct catalytic role of RGS proteins on the GTP hydrolysis of $G\alpha_{i1}$ *in cellulo*, a function that extends beyond merely stabilising Arg-178 for the GTPase reaction as observed with RGS4 [58]. The exact molecular mechanism is open for further studies. Moreover, the $G\alpha_i$ activity may be affected by other factors such as cellular localization and binding to other protein partners including GoLoco proteins, guanine nucleotide dissociation inhibitors, and guanine nucleotide exchange modulators.

Given that Chi1-G183S and Chi1 appeared to associate with the Gβγ dimer to similar degrees (Fig. 5G and H), the binding of Gβγ dimer and RGS proteins to $G\alpha_{i1}$ may not be competitive in nature. This deviates from studies on co-crystal structures of $G\alpha_{i1}$•RGS and $G\alpha_{i1}$•Gβγ [25, 46, 48], wherein the two interfaces overlap. An early FRET-based study suggested that $G\alpha_{i1}$ and Gβγ dimer rearrange, rather than dissociate, upon receptor activation [60]. Such structural rearrangement may be sufficient for RGS proteins to bind to an activated $G\alpha_{i1}$ [61]. This is supported by the current observation that RGS proteins can bind to Chi1 despite having a significant amount of Gβγ dimer associated with the Gα subunit (Fig. 5G and H). Yet, it remains unclear if RGS proteins block AC inhibition by Chi1RC through its GAP activity, or via physical blockade of the AC-interacting surface, as seen with RGS4-inhibition of $G\alpha_q$-mediated PLCβ1 activation by [47]. It should be noted that the coexistence of $G\alpha_{i1}$•RGS and $G\alpha_{i1}$•Gβγ complexes remains possible.

Based on our findings of Chi1NKW, we propose a novel mechanism of AC inhibition by the cooperation between two domains of $G\alpha_{i1\text{-}3}$, including the α3/β5 loop and the region spanning the α4 helix and α4/β6 loop (Fig. 8A, F, and G). The α3/β5 loop is coplanar to the switch II region, and this plane also overlaps with the interacting surfaces of $G\alpha_{i1}$ with Gβγ [48]. Moreover, a recent molecular dynamics study suggested that the C-terminal tip of $G\alpha_{i1}$, which is important for receptor coupling, has strong allosteric modulation towards the Gβγ release from switch II [62]. Therefore, after receptor activation and a pipeline of structural alterations that releases the Gβγ from $G\alpha_{i1}$, the exposed surface is ready for effector recognition. Notably, the α3/β5 loop likely engages in the first binding to the C1 domain of AC, while the plane of α4 helix and α4/β6 loop, which is distant from the α3/β5 loop, may provide a secondary but necessary structural

refinement to elicit AC inhibition, as mutation on the α3/β5 loop alone does not abolish the inhibitory activity completely (Fig. 8A). While the Gβγ released upon receptor activation can also modulate AC activity, we believe that such influence would be minimal since the predominant AC isoforms in HEK293 cells are AC3 and AC6 [63] and they are not activated by Gβγ [64, 65]. Contemporary research on the Gα inhibitory interacting protein (GINIP) indicates that it hinders the interaction between $G\alpha_i$ and adenylyl cyclase, thereby preventing the subsequent modulation of cAMP levels. This inhibition occurs through GINIP binding to the α3/switch II groove of active $G\alpha_i$, which is in proximity to the α3/β5 loop [66]. Additionally, a single point mutation on W258 has been shown to disrupt the binding of GINIP to active $G\alpha_i$ [67]. This suggests that different downstream effectors and modulators of $G\alpha_i$ may competitively bind to this area. Further investigations are required to determine whether the α3/β5 loop region truly functions as an AC interacting site.

In summary, GTPase-deficient (and therefore constitutively active) mutants of $G\alpha_{i1}$ have differential functional resemblance to a receptor-activated $G\alpha_{i1}$. It is due to the distinct ability of RC to be activated by a receptor and to interact with RGS proteins. An additional structural domain, namely the α3/β5 loop, is apparently important for AC inhibition by $G\alpha_{i1\text{-}3}$. Our results provide novel insights on the mechanism of AC inhibition mediated by $G\alpha_i$, as well as deepen our understandings on the properties of two widely used switch region mutants in a cellular context.

Materials and methods

Materials

The cDNAs encoding various human G protein subunits and receptors were obtained from UMR cDNA Resource Center (Rolla, MO, USA). Molecular biology reagents, anti-Flag and Fluo-4 AM were purchased from Invitrogen (Carlsbad, CA, USA). Human embryonic kidney HEK293 cells (CRL-1573) were obtained from American Type Culture Collection (Rockville, MD, USA). Cell culture reagents were obtained from Thermofisher Scientific (Waltham, MA, USA). Polyethylenimine (PEI) (Linear, MW 25,000) was purchased from Polysciences, Inc. (Warrington, PA, USA). Pertussis toxin (PTX) was ordered from List Biological Laboratories (Campbell, CA, USA). Forskolin and quinpirole hydrochloride were purchased from Tocris Bioscience (Bristol, UK). The [^{3}H]adenine was purchased from American Radiolabeled Chemicals (St. Louis, MO, USA) and PerkinElmer (Waltham, MA, USA), while the scintillation fluid (Optiphase Hisafe 3) and [^{3}H]inositol were purchased from PerkinElmer (Waltham, MA, USA). Anti-$G\alpha_{i1}$ primary antibody was from Aviva Systems Biology (San Diego, CA, USA). Anti-$G\alpha_{i2}$ and anti-$G\alpha_{i3}$ antibodies were from Santa Cruz Biotechnology (Santa Cruz, CA, USA). Anti-HA and anti-β-actin were from Roche Molecular Biochemicals (Indianapolis, IN, USA). EZview™ Red ANTI-FLAG® M2 Affinity Gel and other chemicals were purchased from Sigma (St. Louis, MO, USA).

Construction of $G\alpha_i$ mutants

The respective DNA fragments were amplified by polymerase chain reaction (PCR), with the reaction mixture and thermal cycle conditions in accordance with the manufacturer's protocol. Full-length, mutated $G\alpha_{i1}$ cDNA was constructed by overlapping PCR. Primers used for the amplification of fragments are provided in Table 4. The cDNA was cloned into *HindIII* and *XbaI* sites of the pcDNA3.1(+) vector by standard restriction digestion and T4 ligation. Each construct generated was confirmed by Sanger sequencing.

Transient transfection

HEK293 cells were maintained in MEM supplemented with 10% (v/v) of FBS (MEM/FBS), 100 units/mL penicillin and 100 μg/mL streptomycin, incubated at 37 °C in a humidified atmosphere with 5% CO_2. Cells were transiently transfected by PEI transfection system. Briefly, DNA-PEI mixture was prepared by mixing 0.4 μg of plasmid DNA with 50 μL of 150 mM NaCl and 1.6 μL of PEI solution (1 mg/mL). The mixture was vortexed for 10 s and incubated at room temperature for 15 min. Cells in 12-well plates were also fed with 700 μL of fresh MEM/FBS. After 15 min of incubation, 50 μL of DNA-PEI mixture was transferred into each well and was gently mixed. Cells were assayed two days after transfection.

cAMP accumulation assay

Transfected cells were labeled with 1 μCi/mL of [^{3}H] adenine in MEM with 10% (v/v) FBS and treated with 100 ng/mL PTX as appropriate one day after transfection. Labeled cells were challenged in serum-free media with 50 μM forskolin and 1 mM 1-methyl-3-isobutylxanthine, in the absence or presence of 100 nM quinpirole for 30 min. Treatments were terminated by 1 mL of ice-cold stop solution containing 5% (w/v) trichloroacetic acid with 1 mM ATP. Separation of tritiated cAMP from other adenosines was performed by sequential ion

Table 4 List of primers

Construct	Junction/Mutation	Primer sequence (5′ 3′)
Chi1	$G\alpha_{i1}$ $G\alpha_{t1}$ (297–318)	**F:** ATATGTGTTTGATCCTGCATATTCTGG
		R: CCAGAATATGCAGGATCAAACACATATGAGGACGCCGGCAACTAC
		F: GGCACATGTGAAGTGGGTGTATATCTCCTTCACGTCGCGCC
		R: ATATACACCCACTTCACATGTGCC
Chi2 & Chi4	$G\alpha_{i1}$ $G\alpha_{t1}$ (228–236)	**F:** AGCGCCTACGACATGGTGCTAGTGGAGGATGAAGAAATGAACCGAATGC
		R: CTCCACTAGCACCATGTCGTAGGCGCTCAGTGCTACACAGAAGATGATCGCCG
Chi3	$G\alpha_{i1}$ $G\alpha_{t1}$ (297–355)	**F:** CCAGAATATGCAGGATCAAACACATATGAGGACGCCGGCAACTAC
		R: TAGAAGGCACAGTCGAGG
Chi5	$G\alpha_{i1}$ $G\alpha_{q}$ (297–318)	**F:** ATATGTGTTTGATCCTGCATATTCTGG
		R: CCAGAATATGCAGGATCAAACACATATGCCCAGGCAGCCCGAGAATTC
		F: GGCACATGTGAAGTGGGTGTATATAATTTTGTCACTGTCTGG
		R: ATATACACCCACTTCACATGTGCC
Chi6	$G\alpha_{i1}$ $G\alpha_{q}$ (297–349)	**F:** CCAGAATATGCAGGATCAAACACATATGCCCAGGCAGCCCGAGAATTC
		R: CCCTCTAGATTAAAAGAGACCACAATCCTTCAGGTTCAACTGGAGGATGG
Chi1-KH	$G\alpha_{i1}$K248H	**F:** GCATGAAAGCATGCACTTGTTTGACAGC
		R: GCTGTCAAACAAGTGCATGCTTTCATGC
Chi1-DN	$G\alpha_{i1}$D251N	**F:** CATGAAATTGTTTAACAGCATATGTAAC
		R: GTTACATATGCTGTTAAACAATTTCATG
Chi1-KH/DN	$G\alpha_{i1}$K248H/D251N	**F:** GCATGAAAGCATGCACTTGTTTAACAGCATATGTAAC
		R: GTTACATATGCTGTTAAACAAGTGCATGCTTTCATGC
Chi1-KDY, Chi2-KDY, Chi3-KDY	$G\alpha_{i1}$Y287F	**F:** CACTATATGCTTTCCAGAATATGC
		R: GCATATTCTGGAAAGCATATAGTG
Chi1-AAA	$G\alpha_{i1}$E238A/E239A/M240A	**F:** CTAGCTGAAGATGCAGCAGCAAACCGAATGC
		R: GCATTCGGTTTGCTGCTGCATCTTCAGCTAG
$G\alpha_{i1}$-G183S & Chi1-G183S	$G\alpha_{i1}$G183S	**F:** GTGAAAACTACAAGCATTGTTGAAACC
		R: GGTTTCAACAATGCTTGTAGTTTTCAC
$G\alpha_{i1}$-I212A	$G\alpha_{i1}$I212A	**F:** CGGAAGAAGTGGGCTCATTGCTTC
		R: GAAGCAATGAGCCCACTTCTTCCG
$G\alpha_{i1}$-I212L	$G\alpha_{i1}$I212L	**F:** CGGAAGAAGTGGCTTCATTGCTTC
		R: GAAGCAATGAAGCCACTTCTTCCG
$G\alpha_{i1}$-I212V	$G\alpha_{i1}$I212V	**F:** CGGAAGAAGTGGGTTCATTGCTTC
		R: GAAGCAATGAACCCACTTCTTCCG
$G\alpha_{i1}$-I212F	$G\alpha_{i1}$I212F	**F:** CGGAAGAAGTGGTTTCATTGCTTC
		R: GAAGCAATGAAACCACTTCTTCCG
$G\alpha_{i1}$-K209A/I212A	$G\alpha_{i1}$K209A	**F:** GATCTGAGCGGGCGAAGTGGGCTC
		R: GAGCCCACTTCGCCCGCTCAGATC
$G\alpha_{i1}$-NKW or Chi1-NKW	$G\alpha_{i1}$N256H/K257R/W258Y	**F:** GCATATGTAACCACCGCTACTTTACAGATAC
		R: GTATCTGTAAAGTAGCGGTGGTTACATATGC
$G\alpha_{i1}$-K35A	$G\alpha_{i1}$K35A	**F:** CGCGAGGTCGCACTGCTGCTG
		R: CAGCAGCAGTGCGACCTCGCG
$G\alpha_{i1}$-H188A	$G\alpha_{i1}$H188A	**F:** GTTGAAACCGCATTTACTTTC
		R: GAAAGTAAATGCGGTTTCAAC
$G\alpha_{i1}$-K197A	$G\alpha_{i1}$K197A	**F:** CTTCATTTTGCAATGTTTGAT
		R: ATCAAACATTGCAAAATGAAG
$G\alpha_{i1}$-E216A K257A	$G\alpha_{i1}$E216A $G\alpha_{i1}$K257A	**F:** CATTGCTTCGCAGGAGTGACG **R:** CGTCACTCCTGCGAAGCAATG **F:** GTAACAACGCGTGGTTTACAG **R:** CTGTAAACCACGCGTTGTTAC

Table 4 (continued)

Construct	Junction/Mutation	Primer sequence (5′ 3′)
$G\alpha_{i1}$-E216K K257E	$G\alpha_{i1}$E216K $G\alpha_{i1}$K257E	**F:** CATTGCTTCAAAGGAGTGACG **R:** CGTCACTCCTTTGAAGCAATG **F:** GTAACAACGAGTGGTTTACAG **R:** CTGTAAACCACTCGTTGTTAC
$G\alpha_{i1}$-PLT	$G\alpha_{i1}$P282H/T284S	**F:** GCATATGTAACCACCGCTACTTTACAGATAC **R:** GTATCTGTAAAGTAGCGGTGGTTACATATGC
$G\alpha_{i2}$-K210A/I213A	$G\alpha_{i2}$K210A/I213A	**F:** GTCTGAGCGGGCAAAGTGGGCACACTGCTTTG **R:** CAAAGCAGTGTGCCCACTTTGCCCGCTCAGAC
$G\alpha_{i2}$-Chi1-NKW	$G\alpha_{i2}$ $G\alpha_{t1}$ (298–319)	**F:** GCCAACAAATATGAGGACGCCGGCAACTAC **R:** GCCGGCGTCCTCATATTTGTTGGCCCCTGTGTAC **F:** GACGTGAAGGAGATCTACACGCACTTCACG **R:** GTGCGTGTAGATCTCCTTCACGTCGCGCCGCATG
	$G\alpha_{i2}$N257H/K258R/W259Y	**F:** CATCTGCAACCACCGCTACTTCACAGAC **R:** GTCTGTGAAGTAGCGGTGGTTGCAGATG
$G\alpha_{i3}$-CI	$G\alpha_{i3}$C351I	**F:** TAATACGACTCACTATAGGG **R:** GCCCTCTAGACTCGAGTCAATAAAGTCCGATTTCCTTTAAG
$G\alpha_{i3}$-K209A/I212A-CI	$G\alpha_{i3}$K209A/I212A	**F:** GATCAGAACGAGCAAAGTGGGCACACTGTTTTG **R:** CAAAACAGTGTGCCCACTTTGCTCGTTCTGATC
$G\alpha_{i3}$-Chi1-NKW	$G\alpha_{i3}$ $G\alpha_{t1}$ (297–318)	**F:** TCCAATACATATGAGGACGCCGGCAACTAC **R:** GCCGGCGTCCTCATATGTATTGGAACCTGTGTATTC **F:** GACGTGAAGGAGATCTATACTCACTTCACC **R:** GTGAGTATAGATCTCCTTCACGTCGCGCCGCATG
	$G\alpha_{i3}$N256H/K257R/W258Y	**F:** CATTTGTAATCACCGCTACTTTACAGAAAC **R:** GTTTCTGTAAAGTAGCGGTGATTACAAATG

Except $G\alpha_{i2}$-CI and $G\alpha_{i3}$-CI, all mutations to Gα cDNA were made by overlapping PCR using the above primers and the outermost primers (Forward (F): T7 [TAATACGACTCACTATAGGG]; Reverse (R): BGH [TAGAAGGCACAGTCGAGG]), using a template of Gα bearing QL/RC/CI wherever necessary. $G\alpha_{i2}$-CI and $G\alpha_{i3}$-CI were created by direct PCR on $G\alpha_{i2}$ and $G\alpha_{i3}$ cDNA, respectively

exchange chromatography as described previously [19]. The ratios of [^{3}H]cAMP to total [^{3}H]ATP, [^{3}H]ADP, and [^{3}H]cAMP pools were determined. To facilitate comparisons of the inhibitory responses of various chimeras across different experiments, results were expressed as a percentage of forskolin response obtained with the corresponding control, $G\alpha_{i1}$. Absolute values for cAMP accumulation varied between experiments, but cAMP/Total (×1000) values for forskolin-induced responses typically ranged from 80–120; variability within a given experiment was < 10% in general.

Inositol phosphates (IP) accumulation assay

Transfected cells were labeled with 2 μCi/mL of *myo*-[^{3}H] inositol in 10% (v/v) FBS-containing MEM and treated with PTX whenever necessary. Labeled cells were treated with or without 100 nM quinpirole in serum-free media containing 20 mM LiCl for 1 h, and the reaction was stopped by 0.75 mL of 20 mM formic acid. [^{3}H]IP produced was separated from the total [^{3}H]inositol pool by sequential ion exchange chromatography similarly to previous literature [68]. For Ca^{2+} assay, transfectants were transferred into 96-well clear bottom plates and then treated with 100 ng/mL PTX overnight where appropriate. Culture media were then removed followed by cell labeling with 2 μM Fluo-4 AM in HBSS supplemented with 20 mM HEPES (pH 7.5) and 2.5 mM probenecid for 45 min at 37 °C. After the labeling, cells were treated with various doses of quinpirole. Changes in fluorescence were monitored by the FLIPR system with the excitation wavelength of 488 nm as previously described [69].

Western blotting analysis

Transfected cells were lysed by SDS-containing sample buffer (60 mM Tris–HCl (pH 6.8), 5% (v/v) glycerol, 1.7% (w/v) SDS, 1.6% (w/v) dithiothreitol, bromophenol blue). Proteins were separated by 12% SDS–polyacrylamide gel and transferred to nitrocellulose membrane. The membrane was incubated with required antibodies, and chemiluminescence was recorded by the ChemiDoc Touch Imaging System (BioRad, Hercules, CA, USA). Quantification of protein band intensities was performed in ImageJ.

Molecular modeling and sequence alignment

Crystallographic structures were downloaded from the RCSB Protein Data Bank (National Institute of Health, Bethesda, MD, USA), with the PDB codes stated in the figure legends. Alignment of the amino acid sequences of Gα subunit was done by the Clustal Omega multiple sequence alignment program (EMBL-EDI, Hinxton, UK). Analyses on the three-dimensional structures of proteins were performed on PyMOL 2.4.

Molecular Docking of $G\alpha_{i1}$-AC5/6 models using HADDOCK 2.4

To model the interactions between $G\alpha_{i1}$ and AC, the High Ambiguity Driven protein–protein DOCKing software (HADDOCK 2.4) was used, which is accessible at http://wenmr.science.uu.nl/haddock2.4/. The input structures encompassed the AlphaFold-generated structures of human adenylyl cyclase 5 and 6 (Uniprot ID: O95622-1 and O43306-1), along with the X-ray crystallographic structure of $G\alpha_{i1}$ (PDB: 1GFI). The docking process was facilitated through the GURU interface provided by HADDOCK, which requires the inputs of ambiguous interaction restraints (AIRs). AIRs were defined at the binding interface, categorized as "active" and "passive" residues. The "active" residues, informed by experimental data, were directly implicated in the interaction, while the adjacent residues, designated as "passive," were included to account for their close proximity. Subsequent to docking simulations, the model clusters with the lowest HADDOCK scores were further analyzed using PRODIGY and the representative model was visualized using PyMOL 2.4.

Statistical analysis

The cAMP (or IP) levels were calculated as 1000 × [the ratios of the count-per-min of specific fractions ([^{3}H] cAMP or [^{3}H]IP) to those of total fractions ([^{3}H]adenosine phosphates or [^{3}H]inositol). Data shown in the figures were the mean ± SEM of three independent experiments performed in triplicates. The data sets were analyzed by ANOVA and Bonferroni *t* test with 95% confidence. The relative fluorescent unit (RFU) in the Ca^{2+} FLIPR™ assay was calculated by the background-subtracted difference between the maximum and the minimum fluorescence throughout the time course. The corresponding data was expressed as mean ± SD. Data from subunit dissociation assay were represented as mean ± SEM of three individual experiments and was analyzed by Student *t* test. All statistical analyses were performed by GraphPad Prism 8.

Abbreviations

AC	Adenylyl cyclase
cAMP	3′,5′-Cyclic adenosine monophosphate
D_2R	Dopamine D_2 receptor
GAP	GTPase-activating protein
GINIP	Gα inhibitory interacting protein
GPCR	G protein-coupled receptor
GTPγS	Guanosine 5′-O-[γ-thio]-triphosphate
IP	Inositol phosphates
PDEγ	Phosphodiesterase γ
PLCβ	Phospholipase Cβ
PTX	Pertussis toxin
RGS	Regulator of G protein signaling
WT	Wildtype

Supplementary Information

The online version contains supplementary material available at https://doi.org/10.1186/s12964-024-01572-3.

Additional file 1: Fig. S1. Signaling by $G\alpha_{i1/q}$ chimeras. (A) HEK293 cells were transfected with 0.4 μg/mL of various $G\alpha_{i1/t1}$ constructs. Cells were labeled with *myo*-[^{3}H]inositol and then assayed for [^{3}H]IP accumulation. Data shown are mean ± SEM of one triplicate experiment. (B) Expression of $G\alpha_{i1}$ or $G\alpha_q$ constructs were confirmed by immunoblotting with 20 μg of total protein.

Additional file 2: Fig. S2. G_q-signaling by Chi5-CI upon receptor activation. (A) The D_2R-induced IP accumulations of $G\alpha_{i1}$ or $G\alpha_q$ constructs. HEK293 cells were co-transfected with D_2R and various $G\alpha_{i1}$ or $G\alpha_q$ constructs (0.2 μg/mL each), followed by an overnight labeling with *myo*-[^{3}H] inositol and pretreatment with PTX (100 ng/mL) one day after transfection. Cells were assayed for [^{3}H]IP production as in Fig. 4C. Data shown are mean ± SEM of a representative experiment. (B) FLIPR assay on intracellular calcium level upon D_2R stimulation. Transfected cells were labeled with Fluo-4 AM for 45 min, followed by 2-min detection of fluorescence immediately after the application of different concentrations of quinpirole. Data shown are mean ± SEM (*n*=3).

Additional file 3: Fig. S3. Preserved inhibitory function of $G\alpha_{i1}$ in other investigated sites. HEK293 cells were transfected with QL-bearing $G\alpha_{i1}$constructs and assayed as in Fig. 3B. The relative activities of the constitutively active mutants are expressed as a percentage of cAMP accumulation of $G\alpha_{i1}$. Data shown are mean ± SEM (*n*=3). Bonferroni *t* test, $p < 0.05$; †, significant inhibition; #, significantly higher than the control; *, significantly lower than the control.

Additional file 4: Fig. S4. PDBsum prediction on electrostatic interactions on the $G\alpha_{i1}$-AC interface. Predicted hydrogen bonds (in blue solid line), salt bridges (in red solid line), and non-bonded contacts (in orange dashed line) formed between residues of $G\alpha_{i1}$ and (A) AC5 or (B) AC6 are indicated. The filled color represents residue categorization, with blue indicating positive residues (H, K, R), red indicating negative residues (D, E), green indicating neutral residues (S, T, N, Q), gray indicating aliphatic residues (A, V, L, I, M), purple indicating aromatic residues (F, Y, W), brown indicating Proline and Glycine (P, G), and yellow indicating Cysteine (C). Residues subject to mutations are marked with asterisk (*). By comparing (A) and (B), there are several shared interactions between $G\alpha_{i1}$-AC5 and $G\alpha_{i1}$-AC6, which include K209-C485/395, K210-E489/399, H213-M492/402, R208-T555/465, I212-T493/403, K257-L550/460, S252-E553/463, and F215-V554/464.

Acknowledgements

Not applicable.

Authors' contributions

YHW conceptualized the study. All authors designed the experiments. YKC, HYC and TYL performed the experiments. All authors analyzed the data. YKC, HYC and YHW prepared the manuscript. YKC and HYC contributed equally to this work. All authors read and approved the final manuscript.

Funding

This work is supported by grants from the Research Grants Council (16137516 and T13-605/18-W), the University Grants Committee (AoE/M-604/16), and the

Innovation and Technology Commission (ITCPD/17–9) of Hong Kong. YKC was supported by the Deutsche Forschungsgemeinschaft through SFB1423, project number 421152132, subproject A06, during the manuscript preparation.

Availability of data and materials
All data included in this study, information on the materials and methods are available from the corresponding author upon request.

Declarations

Ethics approval and consent to participate
Not applicable.

Consent for publication
Not applicable.

Competing interests
The authors declare no competing interests.

Author details
[1]Division of Life Science and Biotechnology Research Institute, Hong Kong University of Science and Technology, Hong Kong, China. [2]State Key Laboratory of Molecular Neuroscience, and the Molecular Neuroscience Center, Hong Kong University of Science and Technology, Clear Water Bay, Kowloon, Hong Kong, China. [3]Rudolf Schönheimer Institute of Biochemistry, Division of General Biochemistry, Medical Faculty, Leipzig University, Johannisallee 30, 04103 Leipzig, Germany.

Received: 20 January 2024 Accepted: 16 March 2024
Published online: 05 April 2024

References

1. Ho M, Su Y, Yeung W, Wong Y. Regulation of transcription factors by heterotrimeric G Proteins. Curr Mol Pharmacol. 2009;2:19–31.
2. Yim YY, Zurawski Z, Hamm H. GPCR regulation of secretion. Pharmacol Ther. 2018;192:124–40.
3. Cotton M, Claing A. G protein-coupled receptors stimulation and the control of cell migration. Cell Signal. 2009;21:1045–53.
4. New DC, Wong YH. Molecular mechanisms mediating the G protein-coupled receptor regulation of cell cycle progression. J Mol Signal. 2007;2:Art. 2.
5. Darcq E, Kieffer BL. Opioid receptors: drivers to addiction? Nat Rev Neurosci. 2018;19:499–514.
6. Catapano LA, Manji HK. G protein-coupled receptors in major psychiatric disorders. Biochim Biophys Acta (BBA) - Biomembr. 2007;1768:976–93.
7. Svenningsson P, Chergui K, Rachleff I, Flajolet M, Zhang X, Yacoubi ME, et al. Alterations in 5-HT_{1B} Receptor function by p11 in depression-like states. Science. 2006;311:77–80.
8. Massat I, Souery D, Del-Favero J, Gestel SV, Serretti A, Macciardi F, et al. Positive association of dopamine D_2 receptor polymorphism with bipolar affective disorder in a European multicenter association study of affective disorders. Am J Med Genet. 2002;114:177–85.
9. Friedman JI, Adler DN, Temporini HD, Kemether E, Harvey PD, White L, et al. Guanfacine treatment of cognitive impairment in schizophrenia. Neuropsychopharmacol. 2001;25:402–9.
10. Zeng Z, Mukherjee A, Varghese AP, Yang X-L, Chen S, Zhang H. Roles of G protein-coupled receptors in inflammatory bowel disease. World J Gastroenterol. 2020;26:1242–61.
11. de Oliveira PG, Ramos MLS, Amaro AJ, Dias RA, Vieira SI. $G_{i/o}$-Protein Coupled Receptors in the aging brain. Front Aging Neurosci. 2019;11:89.
12. Wang J, Gareri C, Rockman HA. G-Protein–Coupled Receptors in heart disease. Circ Res. 2018;123:716–35.
13. Wong YH, Conklin BR, Bourne HR. G_z-mediated hormonal inhibition of cyclic AMP accumulation. Science. 1992;255:339–42.
14. Wong YH, Federman A, Pace AM, Zachary I, Evans T, Pouysségur J, et al. Mutant α subunits of G_{i2} inhibit cyclic AMP accumulation. Nature. 1991;351:63–5.
15. O'Hara CM, Tang L, Taussig R, Todd RD, O'Malley KL. Dopamine D_{2L} receptor couples to $G\alpha_{i2}$ and $G\alpha_{i3}$ but not $G\alpha_{i1}$, leading to the inhibition of adenylate cyclase in transfected cell lines. J Pharmacol Exp Ther. 1996;278:354–60.
16. Straiker AJ, Borden CR, Sullivan JM. G Protein α subunit isoforms couple differentially to receptors that mediate presynaptic inhibition at rat hippocampal synapses. J Neurosci. 2002;22:2460–8.
17. Medina R, Grishina G, Meloni EG, Muth TR, Berlot CH. Localization of the effector-specifying regions of $G\alpha_{i2}$ and $G\alpha_q$. J Biol Chem. 1996;271:24720–7.
18. Grishina G, Berlot CH. Identification of common and distinct residues involved in the interaction of α_{i2} and α_s with adenylyl cyclase. J Biol Chem. 1997;272:20619–26.
19. Ho MKC, Wong YH. The amino terminus of $G\alpha_z$ is required for receptor recognition, whereas its α4/β6 Loop Is essential for inhibition of adenylyl cyclase. Mol Pharmacol. 2000;58:993–1000.
20. Tesmer JJG, Sunahara RK, Gilman AG, Sprang SR. Crystal structure of the catalytic domains of adenylyl cyclase in a complex with $G\alpha_s$·GTPγS. Science. 1997;278:1907–16.
21. Milano SK, Wang C, Erickson JW, Cerione RA, Ramachandran S. Gain-of-function screen of α-transducin identifies an essential phenylalanine residue necessary for full effector activation. J Biol Chem. 2018;293:17941–52.
22. Evanko DS, Thiyagarajan MM, Takida S, Wedegaertner PB. Loss of association between activated $G\alpha_q$ and Gβγ disrupts receptor-dependent and receptor-independent signaling. Cell Signal. 2005;17:1218–28.
23. Hermouet S, de Mazancourt P, Spiegel AM. Mitogenic effects of pertussis toxin-sensitive G-protein α subunits: The mitogenic action of α_{i2} in NIH 3T3 cells is mimicked by α_{i1}, but not α_{i3}. Cell Signal. 1993;5:215–25.
24. Berman DM, Wilkie TM, Gilman AG. GAIP and RGS4 are GTPase-Activating Proteins for the G_i subfamily of G Protein α subunits. Cell. 1996;86:445–52.
25. Tesmer JJG, Berman DM, Gilman AG, Sprang SR. Structure of RGS4 bound to AlF_4^--activated $G\alpha_{i1}$: Stabilization of the transition state for GTP hydrolysis. Cell. 1997;89:251–61.
26. Chen LT, Gilman AG, Kozasa T. A candidate target for G Protein action in brain. J Biol Chem. 1999;274:26931–8.
27. Skiba NP, Bae H, Hamm HE. Mapping of effector binding sites of Transducin α subunit using $G\alpha_t$/$G\alpha_{i1}$ chimeras. J Biol Chem. 1996;271:413–24.
28. Natochin M, Granovsky AE, Artemyev NO. Identification of effector residues on photoreceptor G Protein. Transducin J Biol Chem. 1998;273:21808–15.
29. Simon MI, Strathmann MP, Gautam N. Diversity of G Proteins in signal transduction. Science. 1991;252:802–8.
30. Berlot CH, Bourne HR. Identification of effector-activating residues of $G\alpha_s$. Cell. 1992;68:911–22.
31. Slep KC, Kercher MA, He W, Cowan CW, Wensel TG, Sigler PB. Structural determinants for regulation of phosphodiesterase by a G protein at 2.0 Å. Nature. 2001;409:1071–7.
32. Conklin BR, Farfel Z, Lustig KD, Julius D, Bourne HR. Substitution of three amino acids switches receptor specificity of $G\alpha_q$ to that of $G\alpha_t$. Nature. 1993;363:274–6.
33. Venkatakrishnan G, Exton JH. Identification of determinants in the α subunit of G_q required for phospholipase C activation. J Biol Chem. 1996;271:5066–72.
34. Freissmuth M, Gilman AG. Mutations of $G\alpha_s$ designed to alter the reactivity of the protein with bacterial toxins: Substitutions at ARG187 result in loss of GTPase activity. J Biol Chem. 1989;264:21907–14.
35. Graziano MP, Gilman AG. Synthesis in *Escherichia coli* of GTPase-deficient mutants of $G\alpha_s$. J Biol Chem. 1989;264:15475–82.
36. Kleuss C, Raw AS, Lee E, Sprang SR, Gilman AG. Mechanism of GTP hydrolysis by G-protein α subunits. Proc Natl Acad Sci. 1994;91:9828–31.
37. Yoshimura M, Cooper DM. Cloning and expression of a Ca^{2+}-inhibitable adenylyl cyclase from NCB-20 cells. Proc Natl Acad Sci. 1992;89:6716–20.
38. Bahia DS, Wise A, Fanelli F, Lee M, Rees S, Milligan G. Hydrophobicity of residue 351 of the G Protein $G\alpha_{i1}$ determines the extent of activation by the α_{2A}-adrenoceptor. Biochemistry. 1998;37:11555–62.
39. Rasmussen SGF, DeVree BT, Zou Y, Kruse AC, Chung KY, Kobilka TS, et al. Crystal structure of the β_2 adrenergic receptor–G_s protein complex. Nature. 2011;477:549–55.

40. Sternweis PC, Gilman AG. Aluminum: a requirement for activation of the regulatory component of adenylate cyclase by fluoride. Proc Natl Acad Sci. 1982;79:4888–91.
41. Noel JP, Hamm HE, Sigler PB. The 2.2 Å crystal structure of transducin-α complexed with GTPγS. Nature. 1993;366:654–63.
42. Coleman D, Berghuis A, Lee E, Linder M, Gilman A, Sprang. Structures of active conformations of $G\alpha_{i1}$ and the mechanism of GTP hydrolysis. Science. 1994;265:1405–12.
43. Goricanec D, Stehle R, Egloff P, Grigoriu S, Plückthun A, Wagner G, et al. Conformational dynamics of a G-protein α subunit is tightly regulated by nucleotide binding. Proc Natl Acad Sci. 2016;113:E3629–38.
44. Landis CA, Masters SB, Spada A, Pace AM, Bourne HR, Vallar L. GTPase inhibiting mutations activate the α chain of G_s and stimulate adenylyl cyclase in human pituitary tumours. Nature. 1989;340:692–6.
45. Lan K-L, Sarvazyan NA, Taussig R, Mackenzie RG, DiBello PR, Dohlman HG, et al. A point mutation in $G\alpha_o$ and $G\alpha_{i1}$ blocks interaction with regulator of g protein signaling proteins. J Biol Chem. 1998;273:12794–7.
46. Soundararajan M, Willard FS, Kimple AJ, Turnbull AP, Ball LJ, Schoch GA, et al. Structural diversity in the RGS domain and its interaction with heterotrimeric G protein α subunits. Proc Natl Acad Sci. 2008;105:6457–62.
47. Hepler JR, Berman DM, Gilman AG, Kozasa T. RGS4 and GAIP are GTPase-activating proteins for $G\alpha_q$ and block activation of phospholipase Cβ by γ-thio-GTP-$G\alpha_q$. Proc Natl Acad Sci. 1997;94:428–32.
48. Wall MA, Coleman DE, Lee E, Iñiguez-Lluhi JA, Posner BA, Gilman AG, et al. The structure of the G protein heterotrimer $G\alpha_{i1}\beta_1\gamma_2$. Cell. 1995;83:1047–58.
49. Dessauer CW, Tesmer JJG, Sprang SR, Gilman AG. Identification of a $G\alpha_i$ binding site on type V adenylyl cyclase. J Biol Chem. 1998;273:25831–9.
50. Qi C, Sorrentino S, Medalia O, Korkhov VM. The structure of a membrane adenylyl cyclase bound to an activated stimulatory G protein. Science. 2019;364:389–94.
51. Zundert GCP van, Rodrigues JPGLM, Trellet M, Schmitz C, Kastritis PL, Karaca E, et al. The HADDOCK2.2 web server: User-friendly integrative modeling of biomolecular complexes. J Mol Biol. 2016;428:720–5.
52. Honorato RV, Koukos PI, Jiménez-García B, Tsaregorodtsev A, Verlato M, Giachetti A, et al. Structural biology in the clouds: The WeNMR-EOSC ecosystem. Front Mol Biosci. 2021;8: 729513.
53. Baldwin TA, Li Y, Brand CS, Watts VJ, Dessauer CW. Insights into the regulatory properties of human adenylyl cyclase type 9. Mol Pharmacol. 2019;95:mol.118.114595.
54. Frezza E, Amans T-M, Martin J. Allosteric inhibition of adenylyl cyclase type 5 by G-Protein: A molecular dynamics study. Biomolecules. 2020;10:1330.
55. Hu Q, Shokat KM. Disease-causing mutations in the G Protein $G\alpha_s$ subvert the roles of GDP and GTP. Cell. 2018;173:1254-1264.e11.
56. Wang J, Ducret A, Tu Y, Kozasa T, Aebersold R, Ross EM. RGSZ1, a Gz-selective RGS protein in brain: Structure, membrane association, regulation by $G\alpha_z$ phosphorylation, and relationship to a G_z GTPase-Activating Protein subfamily. J Biol Chem. 1998;273:26014–25.
57. Masuho I, Balaji S, Muntean BS, Skamangas NK, Chavali S, Tesmer JJG, et al. A global map of G Protein signaling regulation by RGS proteins. Cell. 2020;183:503–521.e19.
58. Mann D, Teuber C, Tennigkeit SA, Schröter G, Gerwert K, Kötting C. Mechanism of the intrinsic arginine finger in heterotrimeric G proteins. Proc Natl Acad Sci. 2016;113:E8041–50.
59. Berman DM, Kozasa T, Gilman AG. The GTPase-activating Protein RGS4 stabilizes the transition state for nucleotide hydrolysis. J Biol Chem. 1996;271:27209–12.
60. Bünemann M, Frank M, Lohse MJ. G_i protein activation in intact cells involves subunit rearrangement rather than dissociation. Proc Natl Acad Sci. 2003;100:16077–82.
61. Chung YK, Wong YH. Re-examining the 'Dissociation Model' of G protein activation from the perspective of Gβγ signaling. FEBS J. 2021;288:2490–501.
62. Hewitt N, Ma N, Arang N, Martin SA, Prakash A, DiBerto JF, et al. Catalytic site mutations confer multiple states of G protein activation. Sci Signal. 2023;16:eabq7842.
63. Soto-Velasquez M, Hayes MP, Alpsoy A, Dykhuizen EC, Watts VJ. A Novel CRISPR/Cas9-Based Cellular Model to Explore Adenylyl Cyclase and cAMP Signaling. Mol Pharmacol. 2018;94:963–72.
64. Tang WJ, Gilman AG. Type-specific regulation of adenylyl cyclase by G protein beta gamma subunits. Science. 1991;254:1500–3.
65. Chan JS, Chiu TT, Wong YH. Activation of type II adenylyl cyclase by the cloned mu-opioid receptor: coupling to multiple G proteins. J Neurochem. 1995;65:2682–9.
66. Luebbers A, Gonzalez-Hernandez AJ, Zhou M, Eyles SJ, Levitz J, Garcia-Marcos M. Dissecting the molecular basis for the modulation of neurotransmitter GPCR signaling by GINIP. Structure. 2024;32:47–59.
67. Park J-C, Luebbers A, Dao M, Semeano A, Nguyen AM, Papakonstantinou MP, et al. Fine-tuning GPCR-mediated neuromodulation by biasing signaling through different G protein subunits. Mol Cell. 2023;83:2540-2558.e12.
68. Chan JSC, Lee JWM, Ho MKC, Wong YH. Preactivation permits subsequent stimulation of phospholipase C by G_i-Coupled Receptors. Mol Pharmacol. 2000;57:700–8.
69. Liu AMF, Ho MKC, Wong CSS, Chan JHP, Pau AHM, Wong YH. $G\alpha_{16/z}$ chimeras efficiently link a wide range of G Protein-Coupled Receptors to calcium mobilization. J Biomol Screen. 2003;8:39–49.

Publisher's Note